ACS Chemical Neuroscience

Review

pubs.acs.org/chemneuro

Intracortical Recording Interfaces: Current Challenges to Chronic Recording Function

Bhagya Gunasekera,[†] Tarun Saxena,[‡] Ravi Bellamkonda,[‡] and Lohitash Karumbaiah*[,†]

[†]Regenerative Bioscience Center, ADS Complex, The University of Georgia, Athens, Georgia 30602-2771, United States

[‡]Wallace H. Coulter Department of Biomedical Engineering, Georgia Institute of Technology, Atlanta, Georgia 30332-0535, United States

ABSTRACT: Brain Computer Interfaces (BCIs) offer significant hope to tetraplegic and paraplegic individuals. This technology relies on extracting and translating motor intent to facilitate control of a computer cursor or to enable fine control of an external assistive device such as a prosthetic limb. Intracortical recording interfaces (IRIs) are critical components of BCIs and consist of arrays of penetrating electrodes that are implanted into the motor cortex of the brain. These multielectrode arrays (MEAs) are responsible for recording and conducting neural signals from local ensembles of neurons in the motor cortex with the high speed and spatiotemporal resolution that is required for exercising control of external assistive prostheses. Recent design and technological innovations in the field have led to significant improvements in BCI function. However, long-term (chronic) BCI function is severely compromised by short-term (acute) IRI recording failure. In this review, we will discuss the design and function of current IRIs. We will also review a host of recent advances that contribute significantly to our overall understanding of the cellular and molecular events that lead to acute recording failure of these invasive implants. We will also present recent improvements to IRI design and provide insights into the futuristic design of more chronically functional IRIs.

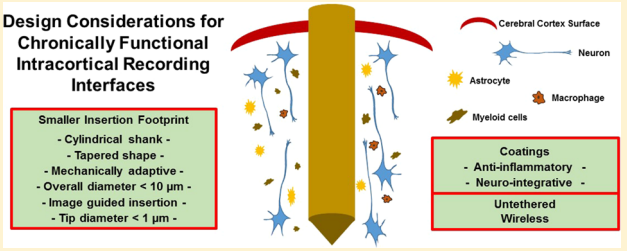

KEYWORDS: *Brain computer interfaces, intracortical neural interfaces, foreign body response*

THE NEED FOR BRAIN COMPUTER INTERFACES

Spinal cord injuries (SCI) and neurodegenerative diseases often lead to severe neurological impairment and permanent incapacitation of individuals that suffer them. Common outcomes include paraplegia, which affects the lower extremities, or tetraplegia, which affects the limbs and torso. In addition to physical incapacitation, the situation is also financially and psychologically burdensome to the individuals, their families, and caregivers. According to The National SCI Statistical Center, around 276 000 people live with SCI in the United States.[1] Around 12 500 new patients suffer SCI in the country each year, with the annual recurring cost ranging from $41 554 for incomplete motor function to $182 033 for high tetraplegia, and estimated lifetime costs ranging from $1 096 770 to $4 651 158.

A number of methods are being used to treat and rehabilitate patients suffering from SCI. Aggressive physiotherapy is a foremost consideration, and has demonstrated considerable success in returning the ability to walk.[2,3] A number of pharmacological interventions such as methylprednisolone have also gained attention over the years, but continue to be the subject of debate for SCI related intervention.[4,5] Immune suppressors such as rapamycin have been used in attempts to mitigate SCI related neural tissue damage in mouse models.[6] Peripheral nerve grafts have shown to promote central nervous system (CNS) axon regeneration,[7] and fetal spinal cord grafts have been used to support regrowth of host axons.[8] More recently, autologous olfactory ensheathing cell transplantation conducted in phase 1 clinical trials have shown promising results in regenerating lesioned axons.[9] Stem cell therapies involving the use of embryonic stem cells, mesenchymal stem cells, neural stem/progenitor cells, and induced pluripotent stem cell transplants have been considered for regenerative therapy of the injured spinal cord.[10−13] Electrical stimulation (ES) of motor neurons has also shown promise in the rehabilitation of patients who have experienced SCI. Intact motor neurons, when electrically stimulated, have been demonstrated to help train paralyzed muscles, reduce muscular atrophy, and improve cardiovascular strength.[14] However, in spite of recent advances, much work remains to be done to achieve the ultimate goal of returning volitional movement to individuals suffering from long-term tetraplegia or paraplegia.

Recently, alternative approaches such as the use of BCIs are being increasingly considered to help return volitional movement to paraplegic or tetraplegic patients. BCIs typically consist of a neural interface (NI), which is capable of recording neural signals from the brain and transmitting them to a computer. The acquired neural signals are subsequently digitized and

Special Issue: Monitoring Molecules in Neuroscience 2014

Received: November 8, 2014
Revised: January 5, 2015
Published: January 14, 2015

DOI: 10.1021/cn5002864
ACS Chem. Neurosci. 2015, 6, 68−83

transmitted via advanced telemetry to an assistive prosthesis that is capable of performing reach and grasp tasks.[15−18] It follows therefore that the ability to reliably record neural signals from populations of neurons in the motor cortex is extremely important for the success of any BCI, and largely depends on the NI employed. Carmena and co-workers developed both open-loop and closed-loop BCI systems, through which monkeys were able to perform reach and grasp tasks using a robotic arm.[19,20] Recent studies have also helped gain a better understanding of the coordination of neural activity leading up to the accomplishment of a motor task, thereby improving predictability of movement.[21] O'Doherty and colleagues demonstrated the use of BCI with a sensory feedback method in rhesus monkey experiments.[22] These studies dawned the concurrent utilization of BCI for motor control and direct intracortical stimulation targeting the sensory cortex. In subsequent studies, Serruya and colleagues demonstrated the ability of rhesus monkeys to track visual targets on a digital screen in a closed-loop BCI.[23] Recent innovations include the development of algorithms used to decode intended movement in real-time,[24] and demonstrate the ability to achieve the performance of reach and grasp tasks by both primates and tetraplegics.[18,19]

From the early recording experiments to the current digitized BCIs, there has been progressive evolution of three BCI components: the NI, information processing system, and the mechanical prostheses. Experiments conducted in primates demonstrated the need to be able to record from large ensembles of neurons in the motor cortex simultaneously, and conduct motor signals to the assistive device.[25] It is therefore critical that the NIs employed for these applications contain a high-density of recording electrodes that can provide reliable chronic recordings with high spatiotemporal resolution.[15,26,27]

INTRACORTICAL RECORDING INTERFACES

Intracortical recording interfaces (IRIs) are microscale recording electrodes implanted into the brain parenchyma. Their primary function is to record and transmit micro- to millivolt scale brain electrical signals from small local neuronal populations in the brain. In early studies, Richard Caton used bare unipolar electrodes and a galvanometer to record brain electrical signals from apes and dogs in 1875.[28] Invasive intracortical electrodes were first used in the mid-1900s in electroshock therapy,[29,30] to record epileptic activity in humans and to perform recording and stimulation of the cat cortex.[31−34] Compared to these approaches, the significantly enhanced signal resolution required for BCI applications depends on two parameters: (a) the number of recording elements; and (b) their proximity to the target neuronal populations. As a result, modern IRIs used for BCI applications possess several improvements in material, size, and recording fidelity. These IRIs are high-density multielectrode arrays (MEAs) that can be implanted with precision and in close proximity to target neuronal populations.

Current NIs can be broadly classified as noninvasive and invasive interfaces. The signal acquisition speed and spatiotemporal signal resolution of NIs used in BCIs are summarized in Figure 1, with a comparison of resultant sensitivity and specificity of recorded signals. Noninvasive electroencephalography (EEG), magnetoencephalography (MEG), and functional magnetic resonance imaging (fMRI) can be used individually or in combination to evaluate neuronal function and to locate areas of aberrant neural activity. These methods demonstrate

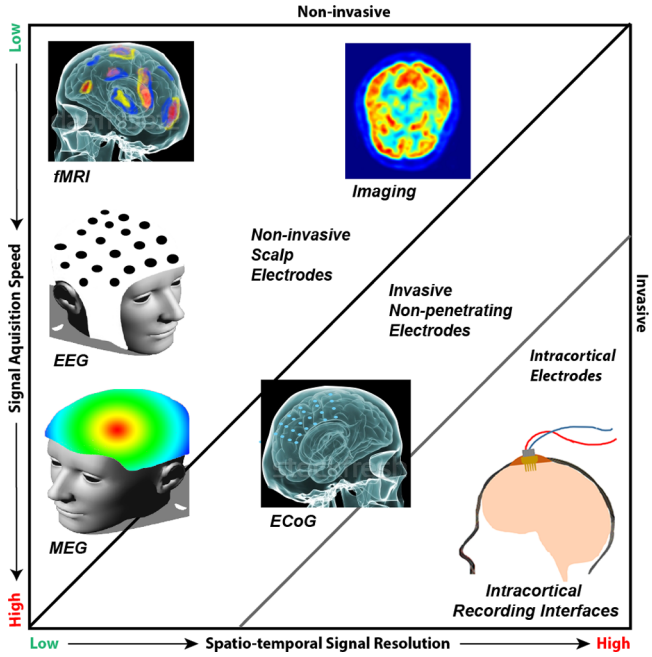

Figure 1. Comparison of recording accuracy and signal acquisition speed between invasive and noninvasive neural interfaces. (Adapted from ref 35.)

low signal acquisition speeds and are used to record gross observations.

Invasive, but nonpenetrating NIs such as electrocorticography (ECoG) arrays demonstrate higher signal acquisition speeds and better signal resolution when compared to noninvasive methods.[36] According to recent reports, these electrodes, when implanted in primates and used in combination with an ECoG-based decoder, showed sufficient signal resolution to perform reach and grasp tasks.[37] In other studies, BCI systems involving high-density 32-electrode ECoG grids have been used successfully to achieve three-dimensional cursor movement and indicate voluntary movement related activation of human sensorimotor cortex.[38] Invasive IRIs consisting of MEAs are capable of recording and conducting neural activity with high signal-to-noise ratios (SNR), because they interface closely with neuronal populations at depths not reachable by other NIs.[39] However, a trade-off of IRIs is the manifestation of acute and chronic complications due to tissue damage and neuronal cell death resulting from their invasive presence in the brain parenchyma. The active lifespan of an IRI is largely dependent on its histocompatibility, which is dictated by a combination of factors such as the material, size, shape, and implantation and tethering modalities.[40−44] Therefore, a detailed understanding of the molecular and cellular events that encompass the foreign body response (FBR) toward chronically implanted IRIs is essential to informing the design of more functional IRIs and is reviewed in subsequent sections.

Current high-density IRIs used for recording applications in rodent, primate, and human studies are listed in Table 1. These interfaces are high-density MEAs that differ from each other primarily in their material, shape, size, recording site placement, and tethering and implantation characteristics.

Figure 2 is a detailed schematic representation of current array design platforms such as the tethered (free-floating) and untethered (rigidly fixed) Michigan microelectrode arrays (MMEA), microwire array (MWA), floating microwire array

DOI: 10.1021/cn5002864
ACS Chem. Neurosci. 2015, 6, 68−83

Table 1. Summary of Application of IRIs in Animal Models and Clinical Trials

IRI platform	dimensions	application
MMEA (untethered)	overall size (including body): 13 mm × 12 mm approx.	rat[45−49]
	shank length: 5 mm approx.	
	shank shape: planar, tapered	
MMEA (tethered)	overall size (including body): 13 mm × 30 mm approx.	
	shank length: 5 mm approx.	
	shank shape: planar, tapered	
MWA (untethered)	overall size (including body): 9 mm × 11 mm approx.	monkey,[22,50,51] mice,[52,53] rat[54−56]
	shank length: 4 mm approx.	
	shank shape: cylindrical, with tapered tip	
FMWA (tethered)	overall size (base): 2 mm × 2.5 mm approx.	
	shank length: 1 mm approx.	
	shank shape: cone	
UEA (tethered)	overall size (base): 2.6 mm × 2.6 mm approx.	rat,[57] monkey,[58] human clinical trials[15,26,27]
	shank length: 1.5 mm approx.	
	shank shape: cone	

(FMWA), and the Utah electrode array (UEA). The design considerations of each individual IRI platform and their respective applications are presented below. Our current understanding of their functional capabilities and the induced FBR are also reviewed.

MICHIGAN ARRAY (MMEA)

Michigan microelectrode arrays are planar silicon based MEAs that present a multishank/multielectrode arrangement. MMEAs present a high electrode density with each of its planar shanks containing multiple recording sites along the length of the shank. Typical geometry and dimensions of untethered MMEAs are depicted in Figure 2A and B. These represent standard four shank MMEAs consisting of shanks that are 5 mm in length, separated by 400 μm spacing, and consisting of planar geometries with 15 μm (Figure 2A) and 50 μm (Figure 2B) shank thickness, respectively. This platform can be configured with multiple electrode recording sites per shank. Untethered electrodes are referred to as such because they lack a flexible "tethering" cable connecting the IRI to the connector. These electrodes consist of the IRI and the connector packaged as a single unit. Untethered electrodes are implanted into the brain parenchyma to desired depths using an insertion tool, and stabilized in place after rigid fixation to the skull (Figure 2G, untethered). In contrast, the tethered

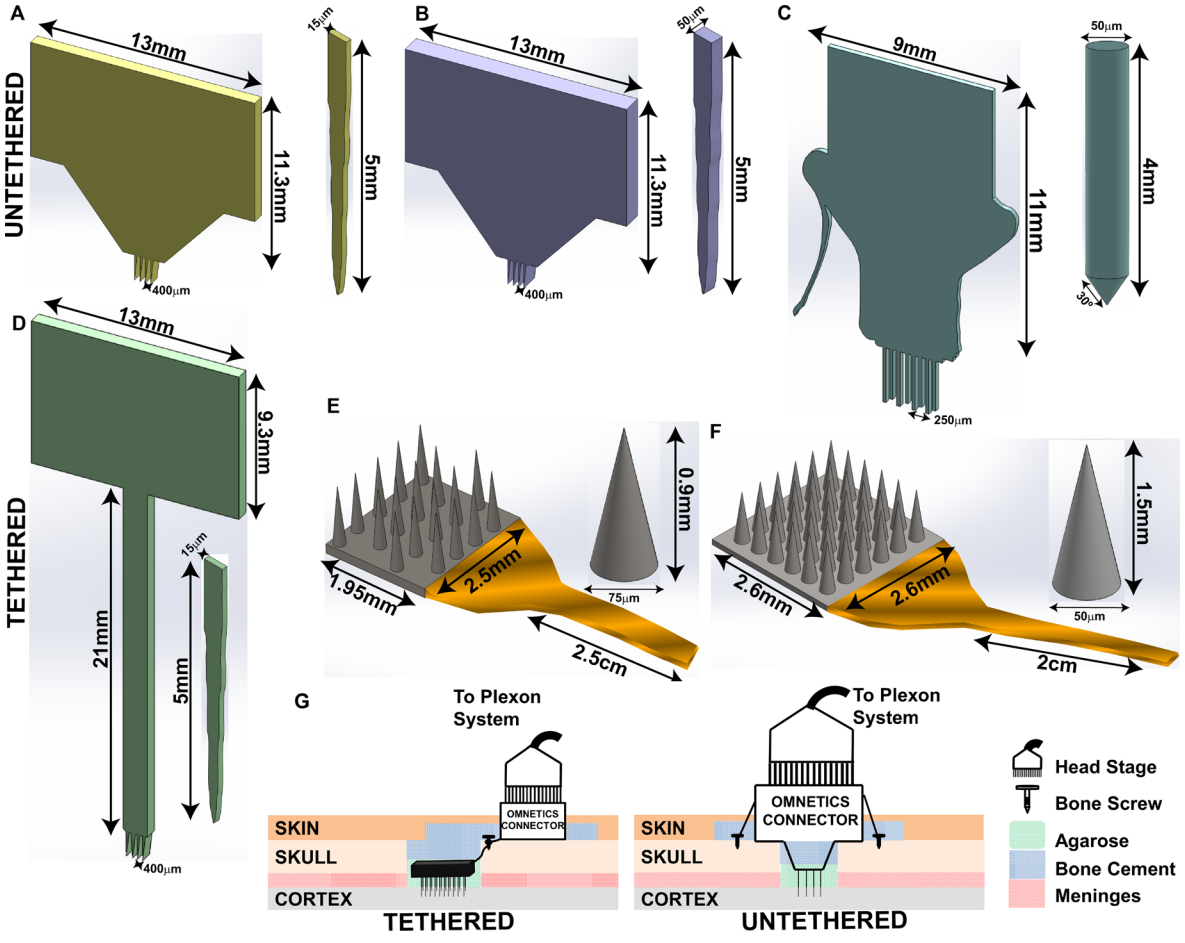

Figure 2. Depiction of intracortical neural interface platforms currently used. Untethered (rigidly fixed) electrodes: (A) MMEA with 15 μm shank; (B) MMEA with 50 μm shank; and (C) MWA. Tethered (free-floating) electrodes: (D) MMEA with 15 μm shank; (E) FMWA; and (F) UEA. Respective dimensions are also depicted alongside MEA platforms. (G) Electrode insertion and headcap placement in the case of tethered and untethered probes is also depicted. Figures do not represent the same scale. (Reprinted with permission from ref 42.)

DOI: 10.1021/cn5002864
ACS Chem. Neurosci. 2015, 6, 68−83

MMEAs (Figure 2D) consist of three distinct components: (1) the IRI, which possesses the same overall characteristics and shank design as the untethered arrays; (2) the flexible cable tether which connects the IRI to the connector; and (3) the connector which is rigidly fixed via dental cement to the skull. The flexible cable tether associated with these electrodes is intended to facilitate "floatation" of the IRI in the brain parenchyma (Figure 2G, tethered), and allow for placement and rigid fixation of the connector on the skull at a location that is distant from the recording site. Although this design is intended to help minimize brain micromotion related tissue response and prolong chronic recording function, evidence from electrode implant studies in small animal models reveals faster recording failure of these interfaces when compared to untethered electrodes as discussed later in this review. MMEAs can range from one shank up to 16 shanks, while each shank may contain upward of four recording sites.[59,60] Recent work on similar design using flexible, shape memory polymer based bioelectronics have also achieved this high recording site density, and have successfully recorded field potentials through 8 weeks in rat auditory cortex.[61] Owing to its arrangement, the MMEA allows simultaneous recording of single unit activity from local neuronal populations, and from different brain layers as desired. Newer, high-density 54-channel array versions have been used to record from large populations of neurons in the cat visual cortex for 3−8 h recording durations.[62] Referred to as polytrodes, these high-density MMEAs are best supported by specifically designed, high-bandwidth data acquisition systems. Owing to improved design, these arrays show minimal crosstalk between channels and low site impedance that lead to better recording accuracy.

Mizuseki and Buzsaki used four- or eight-shank MMEAs to acquire neural recordings simultaneously from multiple layers of the rat hippocampus, and demonstrated differences in synchrony during exploration, rapid-eye-movement sleep, and slow wave sleep.[45] High-density MMEAs were used by Csicsvari and colleagues to obtain massive parallel recording of single unit and local field potentials from the rat hippocampus and somatosensory cortex in acute recording experiments.[46] The micromachined high-density electrodes containing 64 or 96 recording sites used in this study facilitated minimal tissue displacement, and established that action potentials from both soma and dendrites of the same neuron could be simultaneously recorded from. This study demonstrates the MMEAs ability for high-density, high-resolution acute recordings. Rohatgi and colleagues used a 16-channel MMEA coupled with a drug-delivery catheter to facilitate the measurement of individual spikes and local field potentials (LFPs) within the acute time period, and delivery of an infusate containing a mixture of Hoechst dye, propidium iodide, and artificial cerebrospinal fluid simultaneously in the rat primary visual cortex.[63] In other works, MMEAs were implanted in anesthetized rats to simultaneously record LFPs and spikes acutely, while electrically stimulating dopamine overflow.[64] In more recent studies, simultaneous recordings from the auditory cortex and auditory thalamus in rats have been carried out in acute studies using microfabricated titanium based MEAs modeled on the commercial MMEA to record response latencies and isolated action potentials in the separate anatomical sites dedicated for hearing.[47,65] These newer titanium based MEAs demonstrate enhanced fracture toughness, and are potentially compatible with medical imaging techniques such as computer aided tomography (CT) and magnetic resonance imaging (MRI) when compared to conventional silicon based MMEAs. In recent work, optogenetics integration with MMEA has allowed for simultaneous excitation of targeted neurons and acute single unit recording in rat neocortex.[66] Overall, barring a few studies where MMEAs have been demonstrated to provide functional recordings for a period of up to 127 days postimplantation, a vast majority of studies using MMEAs report only the acute functional reliability of MMEAs.[49] In a recent comprehensive evaluation of MMEA function, we report the significantly reduced chronic functionality of different MMEA designs.[42,67] The reasons for acute failure of MMEAs are manifold and are closely related to both electrode design and FBR issues as discussed in later sections of this review.

MICROWIRE ARRAYS (MWA)

Microwires have been used extensively to record neural signals from the brain.[50,68] More recently, applications necessitating the need for chronic neural recordings from anesthetized and behaving animals have employed MWAs.[20,69] Commercially available (Plexon Inc., Microprobes) and newly developed MEAs consist of closely clustered arrangement of 25−50 μm MW shanks, are composed primarily of steel, steel alloys, platinum−iridium or tungsten cores, and are typically insulated in a polymer sheath of polyimide, parylene-C or Teflon.[70−72] Figure 2C schematically represents a typical MWA, alongside which a scaled model of the shank is shown. The tips of the electrodes can be blunt or sharpened as desired. While the sharp tips allow for easy insertion into brain tissue, it exposes more of the metal, thereby lowering the impedance and reducing the ability to record from single neurons.[69] Based on the electrode configuration, the standard MWAs typically consist of 16 fixed position or movable electrodes, or high-density arrays consisting of microwires with different tip lengths to record from different cortical regions.

MWAs have been previously used to record neural activity in awake behaving nonhuman primates.[50] In this study, which employed 704 microwires, 421 single neuronal recordings with a signal-to-noise ratio better than 5:1 were obtained. The study also reports up to 247 cortical neuronal recordings in a single session, and a minimum of 58 isolated single neuronal recordings from one animal 18 months postimplantation. MWAs have also been used to record neuronal action potentials in mice, rats, monkeys, and humans in works that represent both acute and chronic recording periods.[68,69] These studies have demonstrated the acquisition of simultaneous recordings from ensembles of neurons, distributed along different regions, including the cortical and subcortical structures of the brain. The reliability of MWAs to investigate dynamic neuronal interactions that define sensory perception, motor control, and sensorimotor learning has been previously demonstrated in recording intervals spanning several weeks, postimplantation.[68] The ability to record and conduct single unit neural activity is a prerequisite for any IRI communicating with an assistive device such as a prosthetic limb. MWAs implanted in monkeys demonstrated this ability in acute to chronic recording experiments where control of firing rates of single cortical cells improved when volitional control and visual feedback was coupled.[51] In more recent studies, MWAs have been employed to isolate and record from up to 500 cortical neuronal units distributed across multiple cortical areas of a monkey's brain, as proof of MWA's ability to also chronically record large scale brain activity.[73] O'Doherty and colleagues

DOI: 10.1021/cn5002864
ACS Chem. Neurosci. 2015, 6, 68−83

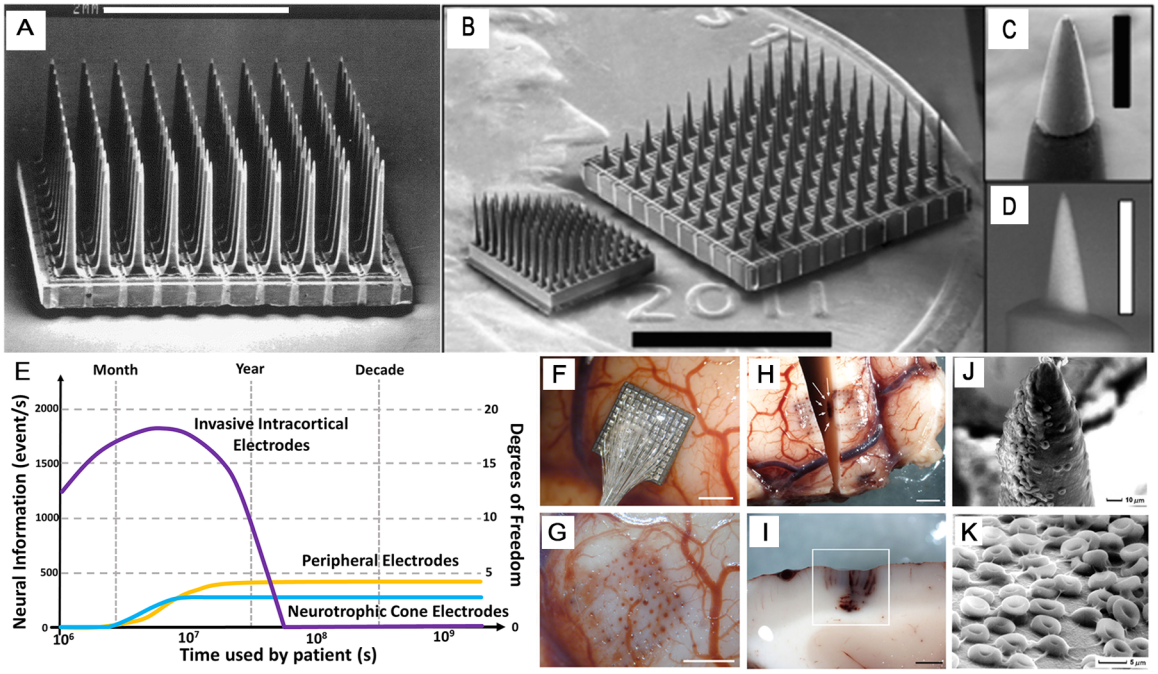

Figure 3. Scanning electron microscopy (SEM) images of a 10 × 10 high-density UEA (A) (scale = 2 mm). Typical USEA platform used commonly for peripheral nerve recording applications (B) (scale = 3 mm). Insets (C) and (D) show, respectively, SEM images of exposed UEA electrode tips achieved via oxygen plasma etching (scale = 50 μm), and through hybrid excimer laser and plasma etching (scale = 25 μm). Plot showing recording fidelity and acute failure of high-density UEAs implanted in humans (purple line) when compared to other interfaces (yellow and blue lines) (E). Image showing UEA implantation in human temporal lobe (F). Image showing microhemorrhage sites after array was removed (G). Horizontal section with petechial hemorrhages observed along electrode tracks (white arrows) (H). Cross section showing the petechial hemorrhages (I). SEM image of an electrode tip showing red blood cells (RBCs) seemingly adsorbed onto the electrode (J). Close-up showing RBCs adsorbed onto the microelectrode surface (K). Scale shown in images (F)−(I) = 2 mm. (Panel (A) reprinted with permission from ref 75. Panels (B)−(D) from ref 57. Panel (E) adapted from DARPA public record. Panels (F)−(K) reprinted with permission from ref 80.)

used four 96 shank MWAs in a monkey to control the exploratory reaching movements of a monkey and provide artificial tactile feedback.[22] This system achieves control of exploratory reaching movement intent, and conducts artificial tactile feedback to the primary somatosensory cortex via intracortical microstimulation, in experiments and preparatory work spanning several weeks. Kumar and colleagues conducted optogenetic stimulation and acquired neural recordings via 32−46 tungsten MWAs implanted in various cortical regions of 4−8 month old Thy1-Chr2 mice to demonstrate activation of cortical projection neurons that regulate oscillatory activity and synchrony.[52] The broader scope of this study is to assess the sufficiency of such stimulation of cortical neurons as a therapeutic strategy for depression. Overall, these experiments tout increased MWA recording reliability and longevity in a broad range of applications.

The floating microwire array (FMWA) platform depicted in Figure 2E is a tethered variant of the MWA. The FMWA consists of a ceramic chip to which multiple microwires of various dimensions can be affixed. Like the aforementioned tethered MMEAs, the FMWA design facilitates movement of the implant along with brain micromotion, and fixation of the connector at a distance from the implant. In early studies, Westby and Wang fabricated and used a custom fabricated FMWA consisting of six 25 μm platinum/iridium wires to record neural signals from the superior colliculus of rats over a period of 5 weeks.[54] Dzirasa and colleagues fabricated FMWAs and obtained up to 70 single units and recorded LFPs simultaneously from 11 brain areas over a period of 16 months postimplantation in mice.[53] In recent studies, we reported stable chronic recording function of MWAs implanted in the rat barrel cortex over a period of 12 weeks postimplantation. In stark contrast, however, we observed acute recording failure of commercial FMWA implants in the same animal model, suggesting that electrode tethering could possibly contribute to mechanical failure of chronically implanted IRIs.[42] Previous reports also suggest that the immune response toward submeninges microwire implants in rats is significantly lower than transmeninges implants, with 63% lower average reactive astrocytes observable on glial scar evaluation.[74]

In summary, a wealth of information points to the use of untethered MWA in chronic applications. A number of design features such as the material, probe shape, and recording site placement may play a key role in facilitating chronic function of these electrodes.

■ UTAH ARRAY (UEA)

The UEA is a micromachined, rigid silicon based high-density array that clusters 100 microelectrodes in a relatively small, approximately 16 mm^2 area of the cortex. Figure 2F depicts a cartoon of a 36 array UEA used commonly in rodent and small animal studies, and Figure 3A depicts a standard 10 × 10 UEA used in primate studies and human trials. Figure 3B depicts a slanted UEA (USEA) which is designed for recording peripheral nerve signals. Figures 3C and D depict recording sites located at the tip of one shank. Standard electrode lengths range from 0.5 to 1.5 mm, while standard electrode pitch is 400 μm for the UEA. The microelectrode at the tip allows for higher signal resolution at each recording point, while the high-density of recording sites are capable of recording neural signals

DOI: 10.1021/cn5002864
ACS Chem. Neurosci. 2015, 6, 68−83

from a large population of cortical neurons. A high-speed, pneumatic insertion mechanism is used for the insertion of implants.

UEAs are critical components of BCIs used in the BrainGate clinical trials.[75,76] In these studies, the ability to restore lost locomotor functions through neuromotor prostheses (NMPs) was explored successfully.[26,77,78] Initial pilot studies demonstrated the ability of a tetraplegic patient implanted in the motor cortex with a 96-electrode UEA to control an external NMP. These preliminary studies provided proof-of-concept and helped demonstrate that volitional intent can be obtained and conducted to an external NMP by an individual 3 years post-SCI. A subsequent study demonstrated the ability of two tetraplegic individuals implanted with UEAs to control robotic arms and perform reach and grasp movements.[15] Importantly, these studies involved volitional control of NMPs without prior training, demonstrating that volitional motor function is never completely lost in individuals that suffer functional CNS deficits. Recent efforts are focused on the design and application of wireless UEAs for a variety of practical reasons including to prevent infection, and chronic mechanical failure resulting from tethering forces and handling of electrode connectors.[40] Zhang and colleagues recently reported the integration of an optical waveguide with a 100 element UEA for simultaneous acute recording and stimulation of mouse brain slices transfected with light sensitive channel protein channelrhodopsin.[79] Although UEAs are capable of recording and conducting high-content neural information required to perform high degree of freedom motor activity, they are prone to acute failure as depicted in Figure 3E. Microhemorrhage of brain tissue vasculature around UEA implants sites, and adhesion of red blood cells to the recording site are depicted in Figures 3F–K.[80] While a variety of biological and nonbiological factors may have contributed to electrode failure, it is likely that the breach of the blood-brain barrier (BBB) and associated pathophysiology may have exacerbated recording failure as discussed later in this review.

The benchmark preclinical UEA studies,[15,26,81] MWA studies,[50,68] and MMEA studies have without a doubt established the IRIs as stable platforms to record single unit neural activity.[82,83] All three platforms also tout successes in neuronal ensembles being recorded, using their respective features, such as the higher electrode density in UEA,[15,26] the multidepth recording multiprobe shanks of MMEA,[45,46,84] and the compact design and stable chronic recording attributes of the MWA platform.[50] Preclinical studies in human patients implanted with the UEA have demonstrated its ability to record the high-content neuronal activity required to control assistive devices.[15,26] However, mounting evidence suggests that these interfaces can be plagued by early recording failure that could compromise BCI function. MWAs have also been used to study the chronic disruption of neural circuitry using genetically modified mouse models,[53] and to record high-content neural activity from primates and humans.[82,83] These and other studies demonstrating the chronic functionality of MWAs point to the potential advantages of using MWAs in BCIs, and should be explored more in a clinical setting. In comparison, the MMEA platform offers a high-density recording interface (64–96 recording sites) via a clustered arrangement of recording sites on relatively few shanks (6–8 shanks). This arrangement can facilitate the acquisition of multilayer recordings while minimizing electrode insertion dependent tissue damage. Markovitz and colleagues used MMEAs for spatial reconstruction of recording sites to associate simultaneous acute multisite recording data obtained from the guinea pig inferior colliculus.[85] Other studies have also demonstrated the ability to conduct massive parallel and simultaneous recording from soma and dendrites of the same neurons with high resolution and with minimal tissue displacement and damage.[46] In spite of these design advantages, MMEAs have predominantly been used in acute studies, and there is little evidence to suggest chronic recording potential of these interfaces. Additionally, the planar design of these IRIs may contribute to shear and strain of brain tissue locally that could exacerbate local inflammatory responses and lead to chronic recording failure.[42]

In addition to the three established platforms, a number of material options have also been explored. Nanowire assemblies have been used to study rat cerebral cortex activity.[86] Silk fibroin based support systems have been used together with ultrathin electrodes in neural mapping studies in the feline brain.[87] Electrodes sandwitched between polyimide layers have been used to study rat brain slices.[88] New fabrication methods have also been used to fabricate flexible high-resolution multiplexed electrode arrays to map brain activity in cats.[89]

MANIFESTATION OF ACUTE AND CHRONIC FOREIGN BODY RESPONSES TO INTRACORTICAL IMPLANTS

Acute insertion dependent damage, as well as acute and chronic FBR to IRIs manifest clinically, and require remedial therapeutic intervention. The mechanical and geometric profile mismatch between the brain and IRI is at the heart of this issue. Previous studies have demonstrated that brain tissue micromotion around stationary indwelling implants in the brain can range between 10 and 30 μm in response to changes in pressure during respiration, and between 2 and 4 μm in response to vascular pulsation.[90] Our current understanding of the acute and chronic responses to IRIs has evolved significantly owing to a wealth of information made available in the recent past, and is reviewed in this section.

Astroglial Scar. Our understanding of the FBR and subsequent recording failure of IRIs is centered around the long-standing dogma that encapsulation of the IRI by reactive astrocytes and microglia results in physical disconnection of the recording interface from the surrounding neuronal populations, and leads to eventual recording failure.[91–94] According to this model, the FBR triggered by IRIs induces the acute activation of resting astrocytes and microglial cells. Termed "reactive gliosis", this response has been histologically demonstrated to be triggered acutely, and is known to ultimately stabilize in the form of compact astroglial scar around chronically implanted IRIs.[42,59,67,84,95,96] Recent studies using two-photon microscopy have also demonstrated the occurrence of this phenomenon in real-time in mouse models.[97] It is believed that the astroglial sheath forms a nonconductive barrier around the implant and leads to the significant attenuation or loss of neural signal.[81,84,96,97] Although the breach of the BBB in response to IRI implants has been described in the past,[55,98–101] the extravasation of blood-borne cells, and the acute and chronic manifestations of this, which include a host of specific cellular and molecular responses that negatively affect neuronal health and IRI recording function, has only recently been elucidated.[67] Figure 4 depicts representative coronal cross sections of a rat cortex implanted with both unmodified and parylene-C coated silicon electrodes. The CD68 immunoreactivity shows macrophage response for a parylene-C coated electrode (Figure 4A).

DOI: 10.1021/cn5002864
ACS Chem. Neurosci. 2015, 6, 68–83

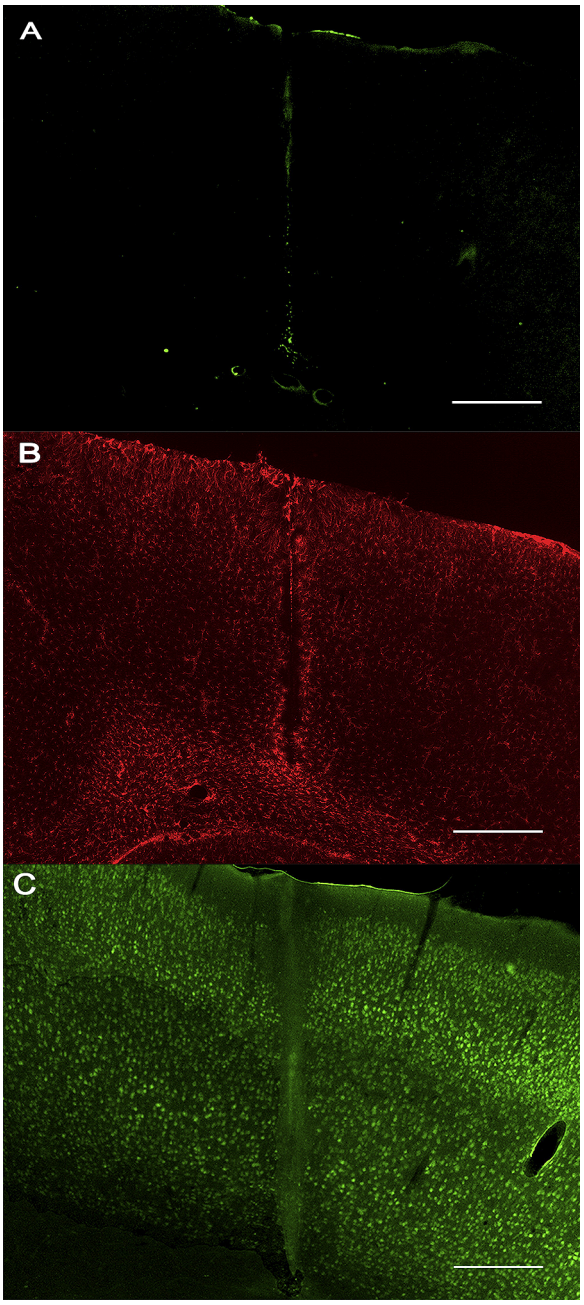

Figure 4. Immunohistochemical staining of coronal rat cortical sections showing the insertion path of a silicon electrode 12 weeks post implantation. (A) Parylene-C coated silicon electrode insertion path showing immunoreactivity for macrophage marker CD68. (B, C) Images showing immunoreactivity for GFAP and NeuN, respectively, along the axis of insertion for an uncoated silicon electrode. Scale = 500 μm. (Reprinted with permission from ref 100.)

The astroglial response to an uncoated electrode is represented by GFAP immunostaining (Figure 4B), and the neuronal population surrounding an uncoated electrode is represented by NeuN immunostaining (Figure 4C).[100]

Acute Response. Studies on murine cortex reveal that neurons and microvesicles assemble within mean distances of around 15 μm between them.[102] With shanks typically exceeding this scale, disruption of microvasculature is imminent. IRI implants are accompanied by a host of events which include insertion dependent tissue damage and neuronal cell death, breach of the BBB, edema, inflammation, neurotoxicity, and the initiation of astroglial scarring.[67] The onset and progression of these events takes place in the minutes to hours postimplantation, which is commonly referred to as the acute injury stage.[42,67] Immediately following the acute injury, the breach of the BBB and concomitant release of erythrocytes, blood-borne cells, clotting factors, neurotoxins, and inflammatory factors into the brain parenchyma leads to the activation of resting astrocytes and microglia.[97] The hypertrophic astrocytes and microglia invade the injury site to remove cell debris, and produce a host of pro- and anti-inflammatory factors to prevent neural tissue damage and promote repair. Although this response is geared toward stabilizing the injury site, the acute mechanical damage of brain tissue, along with the persistent brain tissue micromotion around stationary implants as alluded to earlier, contribute significantly to an exacerbated FBR that is manifested chronically.[42,67]

In recent studies, we subjected astrocytes and microglia to low-magnitude cyclic strain designed to mimic brain micromotion during the respiratory cycle, and demonstrated that acute strain resulted in the significant upregulation of matrix metalloproteinases, reactive gliosis, and proapoptotic factors that could be detrimental to neuronal health.[103] In a subsequently conducted comprehensive analyses of IRI function and implantation induced FBR, we demonstrated that IRI size, shape, and tethering are key factors that differentially influenced acute and chronic inflammatory responses and chronic IRI recording function.[42,67,103]

Chronic Response. The onset of the chronic injury phase begins in the days to weeks postimplantation and continues for as long as the IRI is implanted in the brain tissue. This phase is characterized by a continuation of the astroglial scarring process, which acts as a diffusion barrier to cytokines and serves to protect neuronal populations in the site of injury.[104−106] The mounting astroglial scar eventually ensheaths indwelling IRI and causes recording failure.

Recent studies investigating the biological and nonbiological responses triggered by chronically implanted polyimide insulated 16 shank tungsten MWAs in rats demonstrated structural changes and chronic deterioration of recording sites of electrodes postimplantation (Figure 5).[56] This study evaluated three stages of implant function prior to electrode failure, and hence included three study populations. Figures 5D−F demonstrate structural changes to the recording sites of MWA shanks during the "acute" (hours postimplant; surgery and insertion impact), "recovery" (up to 14 days postimplantation; inflammation impact), and "chronic" (months postimplantation; chronic impact) phases of IRI implantation, respectively.[56] The authors of this study concluded that biological and nonbiological factors were equally responsible for recording failure of MWAs. Combinatorial analysis to demonstrate relationships between biological and nonbiological factors revealed that MWAs in animals with the poorest functional performance demonstrated high electrode impedances and elevated levels of the phosphorylated axonal neurofilament H (pNF-H) subunit.

Until recently, recording failure has been largely attributed to the mounting chronic presence of astroglial scar around invasive recording IRIs. Although astroglial scar is known to harbor nerve inhibitory molecules such as chondroitin sulfate proteoglycans, its major function is to stabilize and prevent further damage to brain tissue, and therefore cannot be the sole mechanism contributing to recording failure. In previous

DOI: 10.1021/cn5002864
ACS Chem. Neurosci. 2015, 6, 68−83

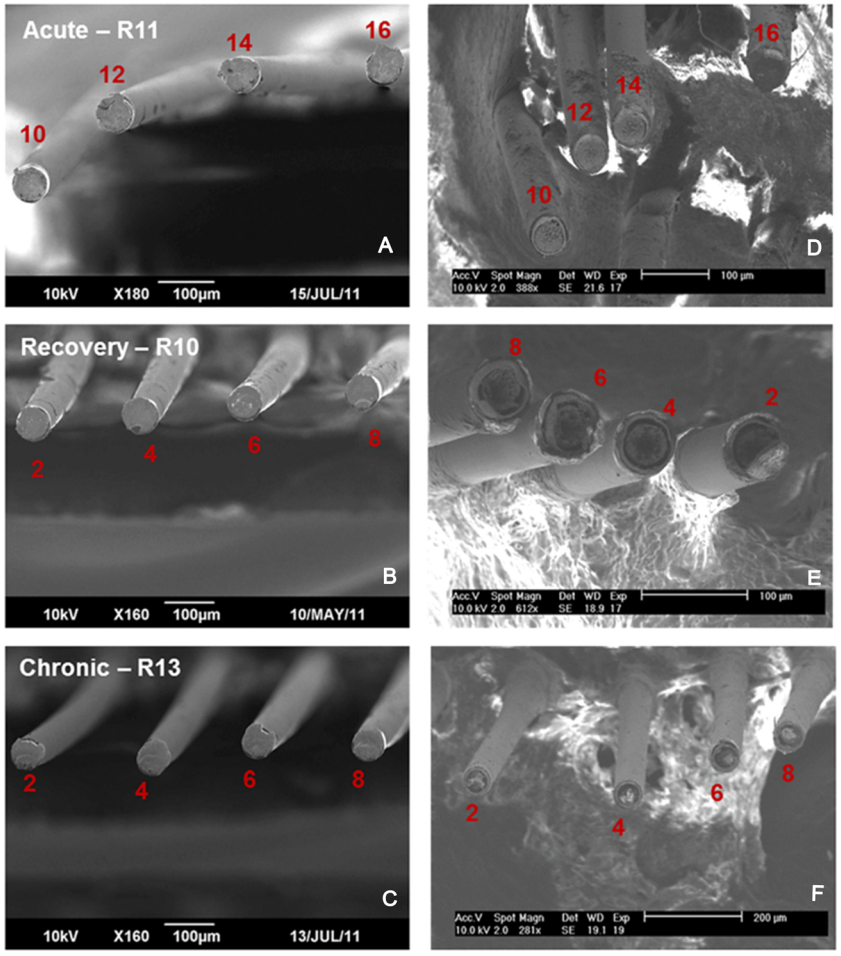

Figure 5. SEM images of selected electrodes from tungsten MWAs implanted in the rat motor cortex. As depicted in the figures (top to bottom), three distinct phases are observed. For each phase, left plane shows preimplant observations, and right plane shows postimplant observations. Images represent structural changes of recording sites and insulation at the end of each of the three phases. Numbers indicate shank and recording site positions. (Reprinted with permission from ref 56.)

studies, we demonstrated that IRIs triggered chronic inflammation, which led to local neurodegeneration of neuronal populations surrounding the implant. In our recent work, we demonstrated that chronic inflammation was associated with increased neuronal and dendritic loss, and not axonal loss.[93] Based on these findings, we sought alternate explanations to the glial scar paradox, and explored the role of the BBB breach in mediating persistent inflammation and neurotoxicity around IRIs used for recording.[67] Using a combination of histological and electrophysiological analyses, we recently demonstrated that untethered MWAs demonstrated a significantly diminished inflammatory response and better electrophysiological function when compared to other tethered and untethered MMEAs, FMWAs, and UEAs at chronic time points (Figure 6).[42,67] Using noninvasive imaging of BBB breach and transcriptomic analysis of neurotoxic cytokines and wound healing markers, we conclusively demonstrated that the markedly better functional performance of MWA can be attributed to significantly reduced breach of the BBB, reduced expression of neurotoxic cytokines, and enhanced wound healing responses chronically.[42,67] In comparing MWAs with the best and worst functional performance, we demonstrated that the chronically functional MWA5 induced a significantly reduced breach of the BBB when compared to MWA3, resulting in enhanced neuronal survival and preservation of recording function chronically (Figure 7). Although the MWA electrodes induced larger insertion dependent neural tissue damage when compared to other IRIs, no abnormal behavior was observed in animals implanted with these electrodes when compared to the others. On the contrary, manual vibrissal stimulation evoked neuronal responses were continually obtained over a period of 16 weeks from animals implanted with these electrodes when compared to others, indicating activity of the barrel cortex circuitry and the chronic functional stability of these interfaces to record neural activity from this region. Figure 7c represents horizontal brain tissue sections obtained from MWA3 and MWA5, and stained for BBB breach using IgG immediately before LCM of tissue. Figure 7d represents NeuN staining of adjacent serial sections, and indicates BBB breach mediated neuronal loss in MWA3 when compared to MWA5. Given the curvature of the rat brain at the region of these implants, it is difficult to hostologically present layer IV specific neuronal populations accurately. However, the whisker stimulation evoked neuronal responses recorded from these chronic implants are indicative of layer IV specificity. Based on these and other findings, we concluded that the prolonged presence and micromotion of invasive IRI induces chronic breach of the BBB, which leads to extravasation of neurotoxic serum proteins into the brain parenchyma. Serum proteins such as albumin and fibrin are known to be neurotoxic and lead to neuronal cell

DOI: 10.1021/cn5002864
ACS Chem. Neurosci. 2015, 6, 68−83

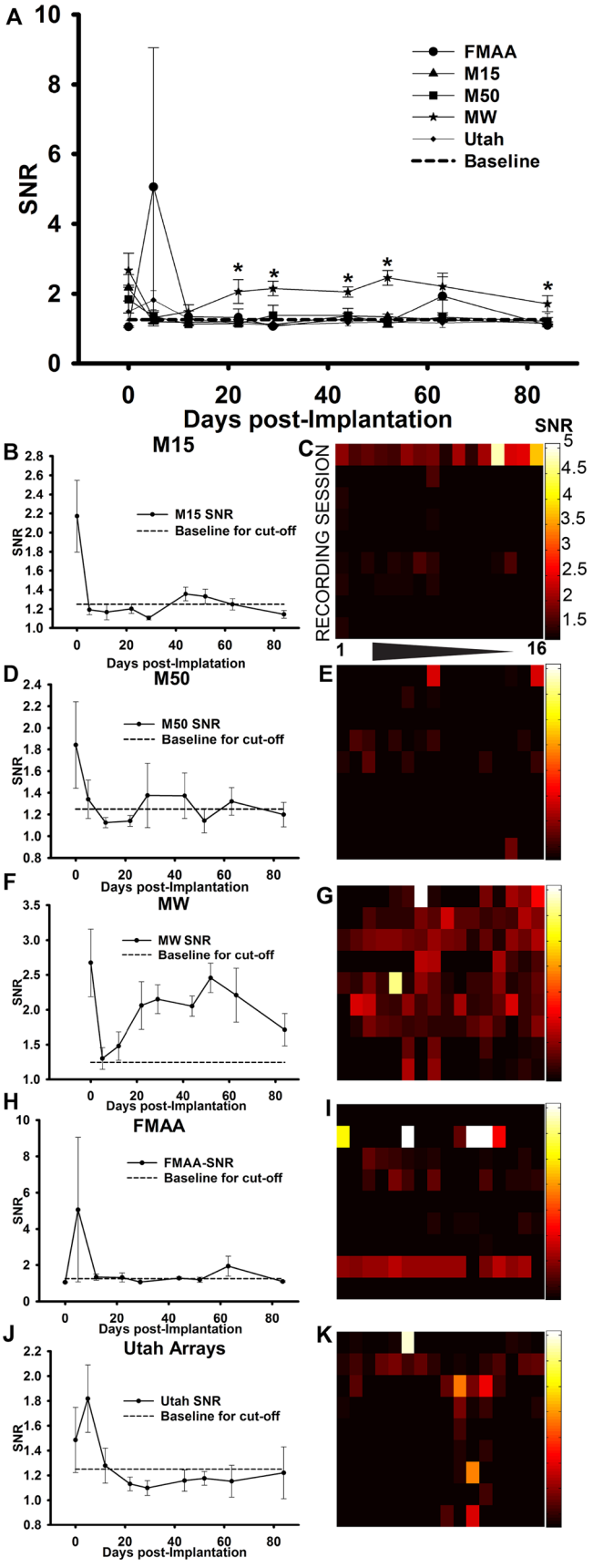

Figure 6. A comparison of SNRs of exoked responses recorded using different IRIs: (A) SNR representation of MMEA 15 μm (M15), MMEA 50 μm (M50), MWA (MW), FMWA (FMA), and UEA (Utah Array) electrodes over a 12 week recording period. Dotted line represents baseline cutoff. Mean values are plotted, with ± S.E.M. (B, D, F, H, and J) Graphs showing SNRs for each platform. (C, E, G, I, and K) Corresponding heat maps representative of each SNR of all 16 channels (abscissa) over each recording session (ordinate) for the respective electrodes as indicated. The heat maps represent the same scale. (Reprinted with permission from ref 42.)

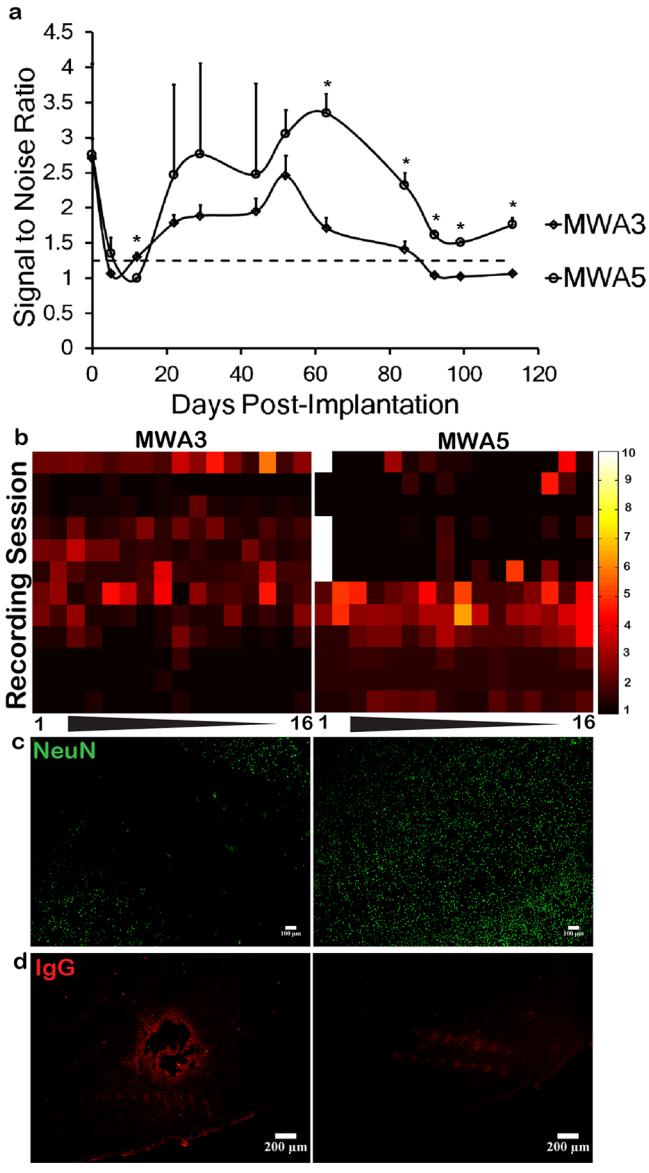

Figure 7. Comparison of best and worst performing MWAs. (a) SNRs of two MWA electrodes, MWA3 (◇) and MWA5 (○), recorded over a period of 16 weeks. Plotted values and mean readings and with ± S.E.M. (b) Comparison of SNRs of individual 16 channels (abscissa) over recording session (ordinate) for each electrode. Heat maps represent the same scale. (c) Representative fluorescent microscopic images of live neurons stained by NeuN staining, showing comparative neuronal abundance around each electrode. (d) Representative fluorescent microscopic images showing the immunoreactivity of rat immunoglobulin-G (IgG) around the two electrodes indicating BBB breach. (Reprinted with permission from ref 67.)

death.[107−109] The situation is also accompanied by the influx of a host of myeloid cells that produce neurotoxic and pro-inflammatory cytokines, which exacerbate reactive gliosis and

DOI: 10.1021/cn5002864
ACS Chem. Neurosci. 2015, 6, 68−83

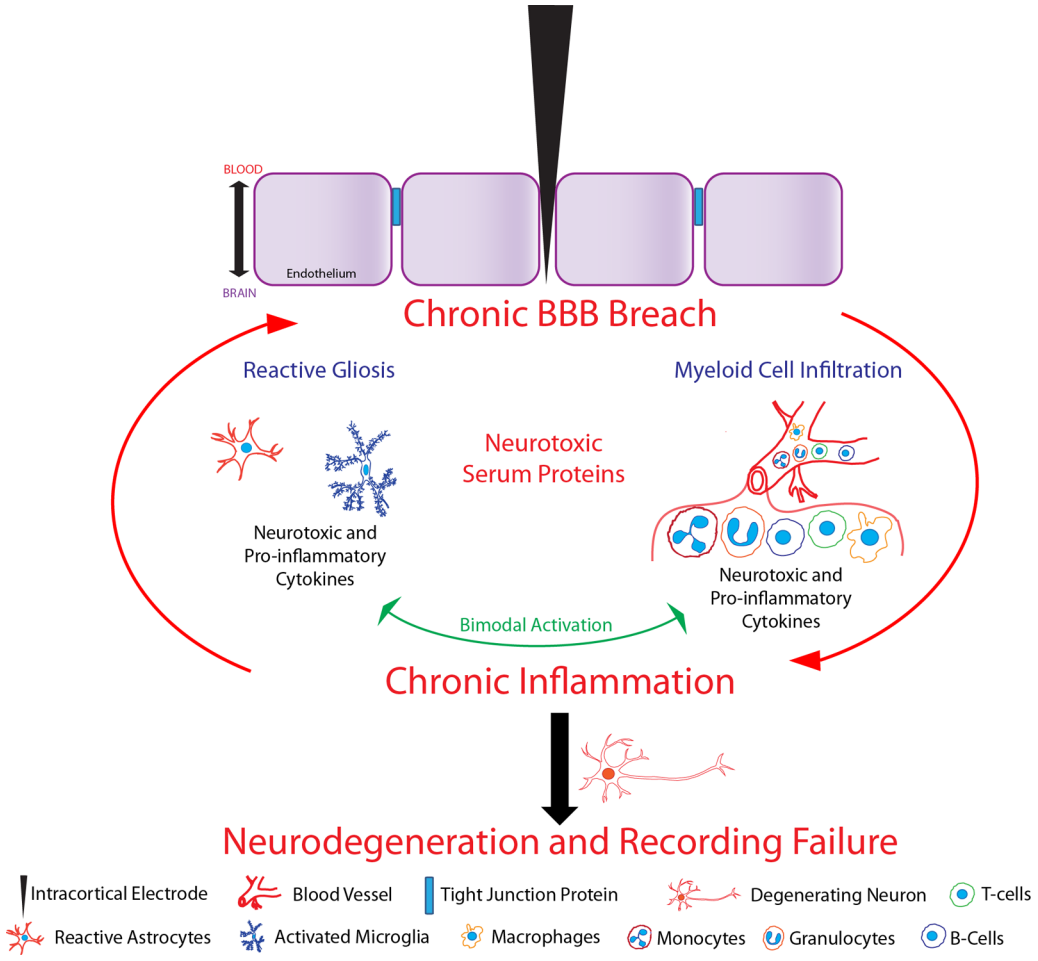

Figure 8. Model depicting BBB breach related mechanisms that lead to chronic electrode failure. Invasive IRIs breach the BBB, resulting in the release of serum proteins, and myeloid cells into the brain parenchyma. Myeloid cell infiltration and reactive gliosis occur concurrently, inducing the release of neurotoxic and inflammatory cytokines. This mechanism ultimately contributes to sustained BBB breach, leading to chronic neurotoxicity and eventual chronic recording failure. (Reprinted with permission from ref 67.)

contribute to chronic neurodegeneration and neurotoxicity, which ultimately leads to recording failure (Figure 8). It is therefore highly likely that issues related to BBB breach as observed in the case of high-density UEA implants in humans (Figure 3F–K) may be significantly contributing to acute recording failure.

STRATEGIES TO PROLONG CHRONIC INTRACORTICAL NEURAL INTERFACE RECORDING FUNCTION

Given our current understanding of the biological and nonbiological responses to chronic indwelling IRIs, a range of strategies are being adopted to help prolong chronic recording performance. These improved IRIs involve improvements to existing design considerations including size, geometric profile and shape, coatings, and materials.

Evidence from literature suggests that IRI insertion footprint and probe size are two key factors that determine the extent of chronic inflammatory response and recording function. Reduced electrode size is therefore an important requirement to help facilitate chronic recording function. Recent reports discuss the feasibility of obtaining intracellular and extracellular recordings using novel carbon nanotube (CNT) probes.[110] These untapered probes are drawn from a multiwalled carbon nanotube solution to a length of ~1 mm and possess a diameter of ~5–10 μm, and a submicrometer tip diameter. These probes demonstrated low impedance and were able to record single-unit neural activity when implanted into the somatosensory cortex of an anesthetized mouse. On similar lines, ultrasmall carbon fiber based microthread electrodes of ~7 μm diameter have been recently developed.[111] These electrodes consisted of a poly(*p*-xylylene)-based thin-film coating which served as a dielectric barrier, and demonstrated single-unit recordings at both acute and chronic time points when implanted into the rat motor cortex.

Bioactive coatings help mitigate FBR to chronically implanted IRIs and potentially prolong chronic recording function. Previously, we have reported the utility of α-melanocyte stimulating hormone (α-MSH) coated IRIs in mitigating acute to chronic glial response for a period of 4 weeks postimplantation in rat brain.[112] We have also reported the deposition of nanoscale coatings consisting of alternating layer-by-layer (LBL) deposition of polycations such as polyethylenimine and chitosan with polyanions such as gelatin and laminin to create neurointegrative interfaces.[113,114] These interfaces demonstrated enhanced neuronal attachment and differentiation in vitro. We also developed nitrocellulose coatings to help facilitate the local delivery of the anti-inflammatory corticosteroid dexamethasone in rat brain.[115] These studies demonstrated the significantly attenuated glial

DOI: 10.1021/cn5002864
ACS Chem. Neurosci. 2015, 6, 68–83

response and enhanced neuronal survival around coated IRIs at acute and chronic time points. In addition to anti-inflammatory and neurointegrative coatings, conductive polymer, carbon nanotube, and hydrogel coatings have been suggested to offer substantial increases in charge transfer area and to help improve IRI performance chronically.[116] Other reports have also suggested the use of thick permeable surface coatings to serve as cytokine diffusion sinks that can help attenuate chronic FBR in vivo.[117] We have previously demonstrated that extracellular matrix (ECM) components such as collagen and amalgams such as polylysine-laminin promote neuronal attachment and differentiation on silicon substrates in vitro and can be useful as neurointegrative coatings.[94] Other strategies to facilitate neurointegration of the probe surface involved immobilization of factors such as nerve growth factor to polypyrrole (PPy) substrates.[118,119] Codeposition of PPy and synthetic peptide DCDPGYIGSR was used to entrap the peptide in PPy layers on chronic implants, limiting diffusion, and leading to the establishment of neural connections in vivo, when implanted in guinea pig brain.[120] However, the same study reported typical glial response and ECM protein reaction after an initial period of obtaining successful recordings from both coated and uncoated probes. Modification of metal electrodes with electrochemically polymerized coatings have also achieved enhanced roughness of surface and low impedance at recording site, and reportedly facilitates preferential attachment of both rat glial cells and human neuroblastoma cells in vitro.[121] Recent reports have also demonstrated the in vitro utility of antioxidative coatings to alleviate chronic degradation of the NI and mitigation of FBR.[122] These studies involved immobilization of the superoxide dismutase mimic Mn(III)tetrakis(4-benzoic acid)-porphyrin on the NI surface, and demonstrated several days of antioxidative activity in the acute phase. Improvements in chronic neural interfacing and chronic recording function have also been studied in vivo using neural adhesion molecule L1 immobilized interfaces.[123,124]

Previous in vitro studies have demonstrated the successful attachment, change in morphology, and proliferation of E9 chicken cortical neurons on silicon wafers coated with collagen-1, polylysine, and laminin.[94] Since laminin alone adhered poorly, these surfaces were initially coated with polylysine and followed by laminin coating to increase adsorption. These preliminary studies demonstrated a modest but significant increase in cell attachment on the collagen and laminin coated surfaces when compared to polylysine and bare silicon surfaces. These studies also demonstrated significantly higher differentiation and formation of interconnections in cells cultured on collagen and laminin coated surfaces when compared to polylysine and bare silicon surfaces. In subsequent in vivo studies, nanoscale laminin functionalized electrodes implanted in the rat cortex for a period of 4 weeks reportedly induced little to no enhancement of neuronal density around the electrode interface, likely due to the lack of neuronal attachment and growth specificity of laminin. However, glial scar related ED-1 and GFAP markers were significantly reduced by ∼20% and ∼50%, respectively, when compared to animals implanted with uncoated electrodes.[113] Although laminin and collagen are ECM proteins capable of promoting neuronal growth and differentiation, the possibility of attachment of other non-neuronal cells has prompted the use of neuron specific cell-adhesion molecules such as L1 protein. Unlike ECM proteins such as laminin, L1 protein belongs to the immunoglobulin family whose expression is tightly regulated during nervous system development. L1 has been demonstrated to promote neuron-to-neuron cell adhesion, and has been reported to promote neural cell adhesion and differentiation in vitro.[123] In recent in vitro studies, L1 protein covalently coupled to silicon wafers seeded with E18 cortical neurons demonstrated a significantly higher neurite outgrowth and reduced astrocyte attachment when compared to silicon wafers coated with laminin,[125] demonstrating the potential of these coatings to promote neuronal attachment and differentiation specifically. These observations were further corroborated in vivo, wherein L1 coated silicon probes implanted in the rat cortex demonstrated significantly increased axonal density, and reduced glial scarring both acutely (1 week) and chronically (4 and 8 weeks) postimplantation.[124] Overall, these studies demonstrate that while ECM coatings can be used effectively to promote cell attachment and differentiation, informed strategies, such as the use of L1 protein coated probes, can help promote neuron specific attachment and outgrowth, and help mitigate reactive gliosis around chronically implanted neuroprostheses.

As discussed earlier, the vast majority of MEAs used in chronic applications are composed of silicon or metallic shanks.[126−132] A variety of materials and composites have since been explored. Composite multiwalled carbon nanotube−polyelectrolyte multilayer electrodes have been demonstrated to outperform electrochemically deposited iridium oxide and poly(3,4-ethylenedioxythiophene) electrodes.[133] The nanotextured surface of the CNT probe was reportedly electrochemically stable, had better charge storage capacities when compared to the other electrodes, and facilitated enhanced adhesion to the underlying substrate. Other surface modifications that could be considered for MEA design involve methods such as deposition of gold on carbon nanofibers.[134] In an attempt to overcome reactive gliosis and demonstrate the feasibility of fabricating a biocompatible interface postinsertion, Wilks and colleagues conducted experiments to demonstrate in vivo polymerization of poly(3,4-ethylenedioxythiophene) (PEDOT) using an electrode-cannula implanted in the rodent cerebral cortex. These studies demonstrated the successful integration of PEDOT, lower impedance, and improved recording quality of local field potentials.[135] In other studies, both PEDOT and PPy nanotubes demonstrated better adherence to silicon dioxide surfaces, and demonstrated reduced impedance and increased charge capacity when compared to films made of the same materials.[136]

Recent reports also discuss the fabrication of novel electrodes designed to help mitigate FBR and prolong chronic electrode function. Kuo and colleagues reported the development of a novel parylene based sheath electrode.[137] These electrodes, the design of which is inspired from previously reported "cone" electrodes,[138−141] present a hollow core to facilitate the ingrowth of neural tissue into the interface. The interface can be lined with neurotrophic factors, and is functionalized with platinum electrodes both on the inside and outside of the device to record neural signals. Wu and colleagues present a high-density 64 channel parylene MEA consisting of a silk backing to provide mechanical support and mitigation of FBR. This MEA which is designed for chronic applications consisted of planar shanks with uniquely placed recording sites that facilitated chronic recording from layer V of the rat motor cortex over a period of 5 weeks postimplantation.[142]

DOI: 10.1021/cn5002864
ACS Chem. Neurosci. 2015, 6, 68−83

FUTURE DESIGN PERSPECTIVES

Successful chronic recording function depends on both acute and chronic management of insertion dependent and micromotion dependent injury and BBB breach, the onset of inflammation, glial scarring, neurodegeneration, and ultimately neurotoxicity and neuronal cell death. The future design of more chronically functional IRIs must take measures to address these issues, and converge upon more sensitive methods of IRI implantation to circumvent BBB breach and mitigate tissue responses that can lead to acute recording failure. While a range of pneumatically actuated and microdive insertion devices are currently available to help facilitate sensitive insertion of IRIs, care should be taken to conduct these procedures under image-guidance to avoid major vascular damage. Recent two-photon imaging studies have indeed demonstrated the acute activation of microglia and vascular damage induced by probe insertion.[97] In vivo two-photon microscopy has also been used to investigate BBB breach and to gain insights on minimizing damage by electrode insertion in cortical neurovasculature of mice,[143] while ex vivo photoacoustic microscopy and MRI have been used to investigate insertion footprints of CNT based microelectrodes in rat motor cortex.[144] Given our recent understanding of the contribution of BBB breach to chronic recording failure, it is important to develop methods to facilitate sensitive image-guided implantation of IRIs in future. A wide range of electrode implantation insertion speeds have also been explored in attempts to limit insertion induced trauma.[84] However, while slow insertion has been demonstrated to allow adjustment of neuronal tissue to the implant and minimize tissue damage,[50] fast electrode insertion has been thought to prevent dural dimping[145] and damage to adjacent tissue.[146] Fast insertion and sharp probes are also known to result in lower overall strain while slower insertion speeds show higher vascular damage in studies conducted ex vivo, using real-time imaging of rat brain slices.[147] Based on recent evidence, the futuristic design of IRIs should incorporate wireless technology and include probes that are reduced in size (<10 μm in diameter); comprise shank geometries that induce minimal strain and shear on surrounding neural tissue; consist of biocompatible, neurointegrative, and anti-inflammatory coatings to help mitigate the FBR and enable chronic recording function; and possess mechanical properties that help facilitate facile insertion and subsequently conform to the modulus of brain tissue. While a number of these strategies are being employed in isolation,[42,103,110−112,148] their collective application in a futuristic device design is currently lacking. Finally, future designs of IRIs should ensure compatibility of IRIs with conventional biomedical imaging techniques such as CT and MRI. These methods can be used effectively to monitor inflammation and BBB breach chronically, and can be used to inform timely therapeutic intervention and prolong chronic recording function.

CONCLUSION

IRIs have significantly evolved from the early application of microwires to record neural signals. Microfabricated high-density IRIs have transformed basic neuroscience research and have helped realize the potential of BCIs as enabling technologies for the severely disabled. In spite of these technological advances, much remains to be done to help better understand the spatiotemporal effects and functional consequences of IRI implants on brain tissue. A host of recent studies have contributed significantly to our collective knowledge on this front, and have helped elucidate the biological and nonbiological factors that contribute to chronic recording failure. Future studies should apply insights gained from these studies to the rational design of more chronically functional IRIs in the near future.

AUTHOR INFORMATION

Corresponding Author

*Mailing address: Regenerative Bioscience Center, ADS Complex, The University of Georgia, 425 River Road, Rm 310, Athens, GA 30602-2771. Tel: 706-542-2017. Fax: 706-583-0274. E-mail: lohitash@uga.edu.

Funding

This work was supported by funding from the Defense Advanced Research Projects Agency (DARPA) MTO under the auspices of Dr. Jack Judy through the Space and Naval Warfare Systems Center, Pacific Grant/Contract No. N66001-11-1-4014 awarded to R.B.

Notes

The authors declare no competing financial interest.

REFERENCES

(1) National Spinal Cord Injury Statistical Center. (2014) *Facts and Figures at a Glance*, University of Alabama, Birmingham AL, https://www.nscisc.uab.edu/PublicDocuments/fact_figures_docs/Facts%202014.pdf (accessed Nov 7, 2014).

(2) Behrman, A. L., and Harkema, S. J. (2000) Locomotor Training After Human Spinal Cord Injury: A Series of Case Studies. *Phys. Ther. 80*, 688−700.

(3) Dobkin, B., Barbeau, H., Deforge, D., Ditunno, J., Elashoff, R., Apple, D., Basso, M., Behrman, A., Harkema, S., Saulino, M., and Scott, M. (2007) The evolution of walking-related outcomes over the first 12 weeks of rehabilitation for incomplete traumatic spinal cord injury: the multicenter randomized Spinal Cord Injury Locomotor Trial. *Neurorehabil. Neural Repair 21*, 25−35.

(4) Bracken, M. B. (2000) Pharmacological interventions for acute spinal cord injury. *Cochrane Database Syst. Rev.*, Cd001046.

(5) Baastrup, C., and Finnerup, N. B. (2008) Pharmacological management of neuropathic pain following spinal cord injury. *CNS Drugs 22*, 455−475.

(6) Sekiguchi, A., Kanno, H., Ozawa, H., Yamaya, S., and Itoi, E. (2012) Rapamycin promotes autophagy and reduces neural tissue damage and locomotor impairment after spinal cord injury in mice. *J. Neurotrauma 29*, 946−956.

(7) Richardson, P. M., McGuinness, U. M., and Aguayo, A. J. (1980) Axons from CNS neurons regenerate into PNS grafts. *Nature 284*, 264−265.

(8) Bregman, B. S., and Reier, P. J. (1986) Neural tissue transplants rescue axotomized rubrospinal cells from retrograde death. *J. Comp Neurol 244*, 86−95.

(9) Tabakow, P., Jarmundowicz, W., Czapiga, B., Fortuna, W., Miedzybrodzki, R., Czyz, M., Huber, J., Szarek, D., Okurowski, S., Szewczyk, P., Gorski, A., and Raisman, G. (2013) Transplantation of autologous olfactory ensheathing cells in complete human spinal cord injury. *Cell Transplant. 22*, 1591−1612.

(10) Thomas, K. E., and Moon, L. D. (2011) Will stem cell therapies be safe and effective for treating spinal cord injuries? *Br. Med. Bull. 98*, 127−142.

(11) Wright, K. T., El Masri, W., Osman, A., Chowdhury, J., and Johnson, W. E. (2011) Concise review: Bone marrow for the treatment of spinal cord injury: mechanisms and clinical applications. *Stem Cells 29*, 169−178.

(12) Enzmann, G. U., Benton, R. L., Talbott, J. F., Cao, Q., and Whittemore, S. R. (2006) Functional considerations of stem cell

DOI: 10.1021/cn5002864
ACS Chem. Neurosci. 2015, 6, 68−83

transplantation therapy for spinal cord repair. *J. Neurotrauma 23*, 479−495.
(13) Tetzlaff, W., Okon, E. B., Karimi-Abdolrezaee, S., Hill, C. E., Sparling, J. S., Plemel, J. R., Plunet, W. T., Tsai, E. C., Baptiste, D., Smithson, L. J., Kawaja, M. D., Fehlings, M. G., and Kwon, B. K. (2011) A systematic review of cellular transplantation therapies for spinal cord injury. *J. Neurotrauma 28*, 1611−1682.
(14) Creasey, G. H., Ho, C. H., Triolo, R. J., Gater, D. R., DiMarco, A. F., Bogie, K. M., and Keith, M. W. (2004) Clinical applications of electrical stimulation after spinal cord injury. *J. Spinal Cord Med. 27*, 365−375.
(15) Hochberg, L. R., Bacher, D., Jarosiewicz, B., Masse, N. Y., Simeral, J. D., Vogel, J., Haddadin, S., Liu, J., Cash, S. S., van der Smagt, P., and Donoghue, J. P. (2012) Reach and grasp by people with tetraplegia using a neurally controlled robotic arm. *Nature 485*, 372−375.
(16) Moritz, C. T., Perlmutter, S. I., and Fetz, E. E. (2008) Direct control of paralysed muscles by cortical neurons. *Nature 456*, 639−642.
(17) Jarosiewicz, B., Chase, S. M., Fraser, G. W., Velliste, M., Kass, R. E., and Schwartz, A. B. (2008) Functional network reorganization during learning in a brain-computer interface paradigm. *Proc. Natl. Acad. Sci. U. S. A. 105*, 19486−19491.
(18) Velliste, M., Perel, S., Spalding, M. C., Whitford, A. S., and Schwartz, A. B. (2008) Cortical control of a prosthetic arm for self-feeding. *Nature 453*, 1098−1101.
(19) Carmena, J. M., Lebedev, M. A., Crist, R. E., O'Doherty, J. E., Santucci, D. M., Dimitrov, D. F., Patil, P. G., Henriquez, C. S., and Nicolelis, M. A. (2003) Learning to control a brain-machine interface for reaching and grasping by primates. *PLoS Biol. 1*, E42.
(20) Lebedev, M. A., Carmena, J. M., O'Doherty, J. E., Zacksenhouse, M., Henriquez, C. S., Principe, J. C., and Nicolelis, M. A. (2005) Cortical ensemble adaptation to represent velocity of an artificial actuator controlled by a brain-machine interface. *J. Neurosci. 25*, 4681−4693.
(21) Afshar, A., Santhanam, G., Yu, B. M., Ryu, S. I., Sahani, M., and Shenoy, K. V. (2011) Single-trial neural correlates of arm movement preparation. *Neuron 71*, 555−564.
(22) O'Doherty, J. E., Lebedev, M. A., Ifft, P. J., Zhuang, K. Z., Shokur, S., Bleuler, H., and Nicolelis, M. A. (2011) Active tactile exploration using a brain-machine-brain interface. *Nature 479*, 228−231.
(23) Serruya, M. D., Hatsopoulos, N. G., Paninski, L., Fellows, M. R., and Donoghue, J. P. (2002) Instant neural control of a movement signal. *Nature 416*, 141−142.
(24) Taylor, D. M., Tillery, S. I., and Schwartz, A. B. (2002) Direct cortical control of 3D neuroprosthetic devices. *Science 296*, 1829−1832.
(25) Georgopoulos, A. P., Schwartz, A. B., and Kettner, R. E. (1986) Neuronal population coding of movement direction. *Science 233*, 1416−1419.
(26) Hochberg, L. R., Serruya, M. D., Friehs, G. M., Mukand, J. A., Saleh, M., Caplan, A. H., Branner, A., Chen, D., Penn, R. D., and Donoghue, J. P. (2006) Neuronal ensemble control of prosthetic devices by a human with tetraplegia. *Nature 442*, 164−171.
(27) Donoghue, J. P., Nurmikko, A., Black, M., and Hochberg, L. R. (2007) Assistive technology and robotic control using motor cortex ensemble-based neural interface systems in humans with tetraplegia. *J. Physiol 579*, 603−611.
(28) Haas, L. F. (2003) Hans Berger (1873−1941), Richard Caton (1842−1926), and electroencephalography. *J. Neurol., Neurosurg. Psychiatry 74*, 9.
(29) Nicolelis, M. (2011) *Beyond boundaries: The new neuroscience of connecting brains with machines—and how it will change our lives*, 1st ed., Times Books/Henry Holt and Co., New York.
(30) Heath, R. G., and Norman, E. C. (1946) Electroshock therapy by stimulation of discrete cortical sites with small electrodes. *Proc. Soc. Exp Biol. Med. 63*, 496−502.
(31) Delgado, J. M. (1952) Permanent implantation of multilead electrodes in the brain. *Yale J. Biol. Med. 24*, 351−358.
(32) Bradley, P. B., and Elkes, J. (1953) A technique for recording the electrical activity of the brain in the conscious animal. *Electroencephalogr. Clin. Neurophysiol. 5*, 451−456.
(33) Vannemreddy, P., Stone, J. L., Vannemreddy, S., and Slavin, K. V. (2010) Psychomotor seizures, Penfield, Gibbs, Bailey and the development of anterior temporal lobectomy: A historical vignette. *Ann. Indian Acad. Neurol. 13*, 103−107.
(34) Hayne, R. A., Belinson, L., and Gibbs, F. A. (1949) Electrical activity of subcortical areas in epilepsy. *Electroencephalogr Clin Neurophysiol 1*, 437−445.
(35) Thakor, N. Building Brain Machine Interfaces − Neuro-prosthetic Control with Electrocorticographic Signals*IEEE Life Sciences Newsletter* , 2012, (April 2012), http://lifesciences.ieee.org/publications/newsletter/april-2012/96-building-brain-machine-interfaces-neuroprosthetic-control-with-electrocorticographic-signals (Accessed Jan 8, 2015).
(36) Hashiguchi, K., Morioka, T., Yoshida, F., Miyagi, Y., Nagata, S., Sakata, A., and Sasaki, T. (2007) Correlation between scalp-recorded electroencephalographic and electrocorticographic activities during ictal period. *Seizure 16*, 238−247.
(37) Chao, Z. C., Nagasaka, Y., and Fujii, N. (2010) Long-term asynchronous decoding of arm motion using electrocorticographic signals in monkeys. *Front. Neuroeng. 3*, 3.
(38) Wang, W., Collinger, J. L., Degenhart, A. D., Tyler-Kabara, E. C., Schwartz, A. B., Moran, D. W., Weber, D. J., Wodlinger, B., Vinjamuri, R. K., Ashmore, R. C., Kelly, J. W., and Boninger, M. L. (2013) An Electrocorticographic Brain Interface in an Individual with Tetraplegia. *PLoS One 8*, e55344.
(39) Santhanam, G., Ryu, S. I., Yu, B. M., Afshar, A., and Shenoy, K. V. (2006) A high-performance brain−computer interface. *Nature 442*, 195−198.
(40) Kim, S., Bhandari, R., Klein, M., Negi, S., Rieth, L., Tathireddy, P., Toepper, M., Oppermann, H., and Solzbacher, F. (2009) Integrated wireless neural interface based on the Utah electrode array. *Biomed. Microdevices 11*, 453−466.
(41) Wester, B. A., Lee, R. H., and LaPlaca, M. C. (2009) Development and characterization of in vivo flexible electrodes compatible with large tissue displacements. *J. Neural Eng. 6*, 024002.
(42) Karumbaiah, L., Saxena, T., Carlson, D., Patil, K., Patkar, R., Gaupp, E. A., Betancur, M., Stanley, G. B., Carin, L., and Bellamkonda, R. V. (2013) Relationship between intracortical electrode design and chronic recording function. *Biomaterials 34*, 8061−8074.
(43) Forcelli, P. A., Sweeney, C. T., Kammerich, A. D., Lee, B. C. W., Rubinson, L. H., Kayinamura, Y. P., Gale, K., and Rubinson, J. F. (2012) Histocompatibility and in vivo signal throughput for PEDOT, PEDOP, P3MT, and polycarbazole electrodes. *J. Biomed. Mater. Res. A 100*, 3455−3462.
(44) Rousche, P. J., Pellinen, D. S., Pivin, D. P., Jr., Williams, J. C., Vetter, R. J., and kirke, D. R. (2001) Flexible polyimide-based intracortical electrode arrays with bioactive capability. *IEEE Trans. Biomed. Eng. 48*, 361−371.
(45) Mizuseki, K., and Buzsaki, G. (2013) Theta oscillations decrease spike synchrony in the hippocampus and entorhinal cortex. *Philos. Trans. R. Soc., B*, B 369.
(46) Csicsvari, J., Henze, D. A., Jamieson, B., Harris, K. D., Sirota, A., Barthó, P., Wise, K. D., and Buzsáki, G. (2003) Massively Parallel Recording of Unit and Local Field Potentials With Silicon-Based Electrodes. *J. Neurophysiol. 90*, 1314−1323.
(47) McCarthy, P. T., Rao, M. P., and Otto, K. J. (2011) Simultaneous recording of rat auditory cortex and thalamus via a titanium-based, microfabricated, microelectrode device. *J. Neural Eng. 8*, 046007.
(48) McCarthy, P. T., Madangopal, R., Otto, K. J., and Rao, M. P. (2009) Titanium-based multi-channel, micro-electrode array for recording neural signals. *Conf. Proc. IEEE Eng. Med. Biol. Soc. 2009*, 2062−2065.

DOI: 10.1021/cn5002864
ACS Chem. Neurosci. 2015, 6, 68−83

(49) Vetter, R. J., Williams, J. C., Hetke, J. F., Nunamaker, E. A., and Kipke, D. R. (2004) Chronic neural recording using silicon-substrate microelectrode arrays implanted in cerebral cortex. *IEEE Trans. Biomed. Eng. 51*, 896−904.
(50) Nicolelis, M. A., Dimitrov, D., Carmena, J. M., Crist, R., Lehew, G., Kralik, J. D., and Wise, S. P. (2003) Chronic, multisite, multielectrode recordings in macaque monkeys. *Proc. Natl. Acad. Sci. U. S. A. 100*, 11041−11046.
(51) Moritz, C. T., and Fetz, E. E. (2011) Volitional control of single cortical neurons in a brain-machine interface. *J. Neural Eng. 8*, 025017.
(52) Kumar, S., Black, S. J., Hultman, R., Szabo, S. T., DeMaio, K. D., Du, J., Katz, B. M., Feng, G., Covington, H. E., 3rd, and Dzirasa, K. (2013) Cortical control of affective networks. *J. Neurosci. 33*, 1116−1129.
(53) Dzirasa, K., Fuentes, R., Kumar, S., Potes, J. M., and Nicolelis, M. A. (2011) Chronic in vivo multi-circuit neurophysiological recordings in mice. *J. Neurosci. Methods 195*, 36−46.
(54) Westby, G. W., and Wang, H. (1997) A floating microwire technique for multichannel chronic neural recording and stimulation in the awake freely moving rat. *J. Neurosci. Methods 76*, 123−133.
(55) Winslow, B. D., and Tresco, P. A. (2010) Quantitative analysis of the tissue response to chronically implanted microwire electrodes in rat cortex. *Biomaterials 31*, 1558−1567.
(56) Prasad, A., Xue, Q. S., Sankar, V., Nishida, T., Shaw, G., Streit, W. J., and Sanchez, J. C. (2012) Comprehensive characterization and failure modes of tungsten microwire arrays in chronic neural implants. *J. Neural Eng. 9*, 056015.
(57) Wark, H. A., Sharma, R., Mathews, K. S., Fernandez, E., Yoo, J., Christensen, B., Tresco, P., Rieth, L., Solzbacher, F., Normann, R. A., and Tathireddy, P. (2013) A new high-density (25 electrodes/mm^2) penetrating microelectrode array for recording and stimulating sub-millimeter neuroanatomical structures. *J. Neural Eng. 10*, 045003.
(58) Dickey, A. S., Suminski, A., Amit, Y., and Hatsopoulos, N. G. (2009) Single-unit stability using chronically implanted multielectrode arrays. *J. Neurophysiol. 102*, 1331−1339.
(59) Biran, R., Martin, D. C., and Tresco, P. A. (2005) Neuronal cell loss accompanies the brain tissue response to chronically implanted silicon microelectrode arrays. *Exp. Neurol. 195*, 115−126.
(60) Ludwig, K. A., Uram, J. D., Yang, J., Martin, D. C., and Kipke, D. R. (2006) Chronic neural recordings using silicon microelectrode arrays electrochemically deposited with a poly(3,4-ethylenedioxythiophene) (PEDOT) film. *J. Neural Eng. 3*, 59−70.
(61) Simon, D., Ware, T., Marcotte, R., Lund, B. R., Smith, D. W., Jr., Di Prima, M., Rennaker, R. L., and Voit, W. (2013) A comparison of polymer substrates for photolithographic processing of flexible bioelectronics. *Biomed. Microdevices 15*, 925−939.
(62) Blanche, T. J., Spacek, M. A., Hetke, J. F., and Swindale, N. V. (2005) Polytrodes: High-Density Silicon Electrode Arrays for Large-Scale Multiunit Recording. *J. Neurophysiol. 93*, 2987−3000.
(63) Rohatgi, P., Langhals, N. B., Kipke, D. R., and Patil, P. G. (2009) In vivo performance of a microelectrode neural probe with integrated drug delivery. *Neurosurg. Focus 27*, E8.
(64) Johnson, M. D., Franklin, R. K., Gibson, M. D., Brown, R. B., and Kipke, D. R. (2008) Implantable microelectrode arrays for simultaneous electrophysiological and neurochemical recordings. *J. Neurosci. Methods 174*, 62−70.
(65) McCarthy, P. T., Otto, K. J., and Rao, M. P. (2011) Robust penetrating microelectrodes for neural interfaces realized by titanium micromachining. *Biomed. Microdevices 13*, 503−515.
(66) Wu, F., Stark, E., Im, M., Cho, I. J., Yoon, E. S., Buzsaki, G., Wise, K. D., and Yoon, E. (2013) An implantable neural probe with monolithically integrated dielectric waveguide and recording electrodes for optogenetics applications. *J. Neural Eng. 10*, 056012.
(67) Saxena, T., Karumbaiah, L., Gaupp, E. A., Patkar, R., Patil, K., Betancur, M., Stanley, G. B., and Bellamkonda, R. V. (2013) The impact of chronic blood-brain barrier breach on intracortical electrode function. *Biomaterials 34*, 4703−4713.
(68) Nicolelis, M. A., Ghazanfar, A. A., Faggin, B. M., Votaw, S., and Oliveira, L. M. (1997) Reconstructing the engram: simultaneous, multisite, many single neuron recordings. *Neuron 18*, 529−537.
(69) Lehew, G., Nicolelis, M. A. L. (2008) State-of-the-Art Microwire Array Design for Chronic Neural Recordings in Behaving Animals, In *Methods for Neural Ensemble Recordings* (Nicolelis, M. A. L., Ed.), 2nd ed., CRC Press, Boca Raton, FL.
(70) Tsai, M. L., and Yen, C. T. (2003) A simple method for fabricating horizontal and vertical microwire arrays. *J. Neurosci. Methods 131*, 107−110.
(71) Weiland, J. D., and Anderson, D. J. (2000) Chronic neural stimulation with thin-film, iridium oxide electrodes. *IEEE Trans. Biomed. Eng. 47*, 911−918.
(72) Cui, G., Jun, S. B., Jin, X., Pham, M. D., Vogel, S. S., Lovinger, D. M., and Costa, R. M. (2013) Concurrent Activation of Striatal Direct and Indirect Pathways During Action Initiation. *Nature 494*, 238−242.
(73) Schwarz, D. A., Lebedev, M. A., Hanson, T. L., Dimitrov, D. F., Lehew, G., Meloy, J., Rajangam, S., Subramanian, V., Ifft, P. J., Li, Z., Ramakrishnan, A., Tate, A., Zhuang, K. Z., and Nicolelis, M. A. L. (2014) Chronic, wireless recordings of large-scale brain activity in freely moving rhesus monkeys. *Nat. Methods 11*, 670−676.
(74) Markwardt, N. T., Stokol, J., and Rennaker Ii, R. L. (2013) Sub-meninges implantation reduces immune response to neural implants. *J. Neurosci. Methods 214*, 119−125.
(75) Normann, R. A., Maynard, E. M., Rousche, P. J., and Warren, D. J. (1999) A neural interface for a cortical vision prosthesis. *Vision Res. 39*, 2577−2587.
(76) Normann, R. A., Campbell, P. K., and Jones, K. E. (1993) Three-dimensional electrode device. U.S. Patent US5215088 A.
(77) Homer, M. L., Nurmikko, A. V., Donoghue, J. P., and Hochberg, L. R. (2013) Sensors and decoding for intracortical brain computer interfaces. *Annu. Rev. Biomed. Eng. 15*, 383−405.
(78) Perge, J. A., Homer, M. L., Malik, W. Q., Cash, S., Eskandar, E., Friehs, G., Donoghue, J. P., and Hochberg, L. R. (2013) Intra-day signal instabilities affect decoding performance in an intracortical neural interface system. *J. Neural Eng. 10*, 036004.
(79) Zhang, J., Laiwalla, F., Kim, J. A., Urabe, H., Van Wagenen, R., Song, Y. K., Connors, B. W., Zhang, F., Deisseroth, K., and Nurmikko, A. V. (2009) Integrated device for optical stimulation and spatiotemporal electrical recording of neural activity in light-sensitized brain tissue. *J. Neural Eng. 6*, 055007.
(80) Fernandez, E., Greger, B., House, P. A., Aranda, I., Botella, C., Albisua, J., Soto-Sanchez, C., Alfaro, A., and Normann, R. A. (2014) Acute human brain responses to intracortical microelectrode arrays: Challenges and future prospects. *Front. Neuroeng.*, DOI: 10.3389/fneng.2014.00024.
(81) Schwartz, A. B. (2004) Cortical neural prosthetics. *Annu. Rev. Neurosci. 27*, 487−507.
(82) Patil, P. G., Carmena, J. M., Nicolelis, M. A., and Turner, D. A. (2004) Ensemble recordings of human subcortical neurons as a source of motor control signals for a brain-machine interface. *Neurosurgery 55*, 27−38.
(83) Wessberg, J., Stambaugh, C. R., Kralik, J. D., Beck, P. D., Laubach, M., Chapin, J. K., Kim, J., Biggs, S. J., Srinivasan, M. A., and Nicolelis, M. A. (2000) Real-time prediction of hand trajectory by ensembles of cortical neurons in primates. *Nature 408*, 361−365.
(84) Polikov, V. S., Tresco, P. A., and Reichert, W. M. (2005) Response of brain tissue to chronically implanted neural electrodes. *J. Neurosci Methods 148*, 1−18.
(85) Markovitz, C. D., Tang, T. T., Edge, D. P., and Lim, H. H. (2012) Three-dimensional brain reconstruction of in vivo electrode tracks for neuroscience and neural prosthetic applications. *Front. Neural Circuits 6*, 39.
(86) Suyatin, D. B., Wallman, L., Thelin, J., Prinz, C. N., Jorntell, H., Samuelson, L., Montelius, L., and Schouenborg, J. (2013) Nanowire-based electrode for acute in vivo neural recordings in the brain. *PLoS One 8*, e56673.
(87) Kim, D.-H., Viventi, J., Amsden, J. J., Xiao, J., Vigeland, L., Kim, Y.-S., Blanco, J. A., Panilaitis, B., Frechette, E. S., Contreras, D., Kaplan,

DOI: 10.1021/cn5002864
ACS Chem. Neurosci. 2015, 6, 68−83

D. L., Omenetto, F. G., Huang, Y., Hwang, K.-C., Zakin, M. R., Litt, B., and Rogers, J. A. (2010) Dissolvable films of silk fibroin for ultrathin conformal bio-integrated electronics. *Nat. Mater. 9*, 511−517.
(88) Boppart, S. A., Wheeler, B. C., and Wallace, C. S. (1992) A flexible perforated microelectrode array for extended neural recordings. *IEEE Trans. Biomed. Eng. 39*, 37−42.
(89) Viventi, J., Kim, D.-H., Vigeland, L., Frechette, E. S., Blanco, J. A., Kim, Y.-S., Avrin, A. E., Tiruvadi, V. R., Hwang, S.-W., Vanleer, A. C., Wulsin, D. F., Davis, K., Gelber, C. E., Palmer, L., Van der Spiegel, J., Wu, J., Xiao, J., Huang, Y., Contreras, D., Rogers, J. A., and Litt, B. (2011) Flexible, foldable, actively multiplexed, high-density electrode array for mapping brain activity in vivo. *Nat. Neurosci. 14*, 1599−1605.
(90) Gilletti, A., and Muthuswamy, J. (2006) Brain micromotion around implants in the rodent somatosensory cortex. *J. Neural Eng. 3*, 189−195.
(91) Carulli, D., Laabs, T., Geller, H. M., and Fawcett, J. W. (2005) Chondroitin sulfate proteoglycans in neural development and regeneration. *Curr. Opin. Neurobiol. 15*, 116−120.
(92) Grill, W. M., Norman, S. E., and Bellamkonda, R. V. (2009) Implanted neural interfaces: Biochallenges and engineered solutions. *Annu. Rev. Biomed. Eng. 11*, 1−24.
(93) McConnell, G. C., Rees, H. D., Levey, A. I., Gutekunst, C. A., Gross, R. E., and Bellamkonda, R. V. (2009) Implanted neural electrodes cause chronic, local inflammation that is correlated with local neurodegeneration. *J. Neural Eng. 6*, 056003.
(94) Zhong, Y., Yu, X., Gilbert, R., and Bellamkonda, R. V. (2001) Stabilizing electrode-host interfaces: A tissue engineering approach. *J. Rehabil. Res. Dev. 38*, 627−632.
(95) Biran, R., Martin, D. C., and Tresco, P. A. (2007) The brain tissue response to implanted silicon microelectrode arrays is increased when the device is tethered to the skull. *J. Biomed. Mater. Res., Part A 82*, 169−178.
(96) McConnell, G. C., Schneider, T. M., and Bellamkonda, R. V. (2007) Acute spatiotemporal changes in neuronal density surrounding microelectrode arrays implanted in rat motor cortex. *3rd Int IEEE/EMBS Conf. Neural Eng., 2007. CNE '07*, 137−140.
(97) Kozai, T. D., Vazquez, A. L., Weaver, C. L., Kim, S. G., and Cui, X. T. (2012) In vivo two-photon microscopy reveals immediate microglial reaction to implantation of microelectrode through extension of processes. *J. Neural Eng. 9*, 066001.
(98) Seymour, J. P., and Kipke, D. R. (2007) Neural probe design for reduced tissue encapsulation in CNS. *Biomaterials 28*, 3594−3607.
(99) Szarowski, D. H., Andersen, M. D., Retterer, S., Spence, A. J., Isaacson, M., Craighead, H. G., Turner, J. N., and Shain, W. (2003) Brain responses to micro-machined silicon devices. *Brain Res. 983*, 23−35.
(100) Winslow, B. D., Christensen, M. B., Yang, W. K., Solzbacher, F., and Tresco, P. A. (2010) A comparison of the tissue response to chronically implanted Parylene-C-coated and uncoated planar silicon microelectrode arrays in rat cortex. *Biomaterials 31*, 9163−9172.
(101) Spataro, L., Dilgen, J., Retterer, S., Spence, A. J., Isaacson, M., Turner, J. N., and Shain, W. (2005) Dexamethasone treatment reduces astroglia responses to inserted neuroprosthetic devices in rat neocortex. *Exp. Neurol. 194*, 289−300.
(102) Tsai, P. S., Kaufhold, J. P., Blinder, P., Friedman, B., Drew, P. J., Karten, H. J., Lyden, P. D., and Kleinfeld, D. (2009) Correlations of Neuronal and Microvascular Densities in Murine Cortex Revealed by Direct Counting and Colocalization of Nuclei and Vessels. *J. Neurosci. 29*, 14553−14570.
(103) Karumbaiah, L., Norman, S. E., Rajan, N. B., Anand, S., Saxena, T., Betancur, M., Patkar, R., and Bellamkonda, R. V. (2012) The upregulation of specific interleukin (IL) receptor antagonists and paradoxical enhancement of neuronal apoptosis due to electrode induced strain and brain micromotion. *Biomaterials 33*, 5983−5996.
(104) Saxena, T., Gilbert, J., Stelzner, D., and Hasenwinkel, J. (2012) Mechanical characterization of the injured spinal cord after lateral spinal hemisection injury in the rat. *J. Neurotrauma 29*, 1747−1757.
(105) Fawcett, J. W., and Asher, R. A. (1999) The glial scar and central nervous system repair. *Brain Res. Bull. 49*, 377−391.
(106) Karumbaiah, L., and Bellamkonda, R. (2013) Neural Tissue Engineering, In *Neural Engineering* (He, B., Ed.), pp 765−794, Springer, New York.
(107) Hassel, B., Iversen, E. G., and Fonnum, F. (1994) Neurotoxicity of albumin in vivo. *Neurosci. Lett. 167*, 29−32.
(108) Matz, P. G., Lewen, A., and Chan, P. H. (2001) Neuronal, but not microglial, accumulation of extravasated serum proteins after intracerebral hemolysate exposure is accompanied by cytochrome c release and DNA fragmentation. *J. Cereb. Blood Flow Metab. 21*, 921−928.
(109) Paul, J., Strickland, S., and Melchor, J. P. (2007) Fibrin deposition accelerates neurovascular damage and neuroinflammation in mouse models of Alzheimer's disease. *J. Exp. Med. 204*, 1999−2008.
(110) Yoon, I., Hamaguchi, K., Borzenets, I. V., Finkelstein, G., Mooney, R., and Donald, B. R. (2013) Intracellular Neural Recording with Pure Carbon Nanotube Probes. *PLoS One 8*, e65715.
(111) Kozai, T. D., Langhals, N. B., Patel, P. R., Deng, X., Zhang, H., Smith, K. L., Lahann, J., Kotov, N. A., and Kipke, D. R. (2012) Ultrasmall implantable composite microelectrodes with bioactive surfaces for chronic neural interfaces. *Nat. Mater. 11*, 1065−1073.
(112) He, W., McConnell, G. C., Schneider, T. M., and Bellamkonda, R. V. (2007) A novel anti-inflammatory surface for neural electrodes. *Adv. Mater. 19*, 3529−+.
(113) He, W., McConnell, G. C., and Bellamkonda, R. V. (2006) Nanoscale laminin coating modulates cortical scarring response around implanted silicon microelectrode arrays. *J. Neural Eng. 3*, 316−326.
(114) Crompton, K. E., Goud, J. D., Bellamkonda, R. V., Gengenbach, T. R., Finkelstein, D. I., Horne, M. K., and Forsythe, J. S. (2007) Polylysine-functionalised thermoresponsive chitosan hydrogel for neural tissue engineering. *Biomaterials 28*, 441−449.
(115) Zhong, Y., and Bellamkonda, R. V. (2007) Dexamethasone-coated neural probes elicit attenuated inflammatory response and neuronal loss compared to uncoated neural probes. *Brain Res. 1148*, 15−27.
(116) Aregueta-Robles, U. A., Woolley, A. J., Poole-Warren, L. A., Lovell, N. H., and Green, R. A. (2014) Organic electrode coatings for next-generation neural interfaces. *Front. Neuroeng. 7*, 15.
(117) Skousen, J. L., Bridge, M. J., and Tresco, P. A. (2015) A strategy to passively reduce neuroinflammation surrounding devices implanted chronically in brain tissue by manipulating device surface permeability. *Biomaterials 36*, 33−43.
(118) Kim, D. H., Richardson-Burns, S. M., Hendricks, J. L., Sequera, C., and Martin, D. C. (2007) Effect of immobilized nerve growth factor on conductive polymers: Electrical properties and cellular response. *Adv. Funct. Mater. 17*, 79−86.
(119) Gomez, N., and Schmidt, C. E. (2007) Nerve growth factor-immobilized polypyrrole: Bioactive electrically conducting polymer for enhanced neurite extension. *J. Biomed. Mater. Res., Part A 81A*, 135−149.
(120) Cui, X., Wiler, J., Dzaman, M., Altschuler, R. A., and Martin, D. C. (2003) In vivo studies of polypyrrole/peptide coated neural probes. *Biomaterials 24*, 777−787.
(121) Cui, X., Lee, V. A., Raphael, Y., Wiler, J. A., Hetke, J. F., Anderson, D. J., and Martin, D. C. (2001) Surface modification of neural recording electrodes with conducting polymer/biomolecule blends. *J. Biomed. Mater. Res. 56*, 261−272.
(122) Potter-Baker, K. A., Nguyen, J. K., Kovach, K. M., Gitomer, M. M., Srail, T. W., Stewart, W. G., Skousen, J. L., and Capadona, J. R. (2014) Development of Superoxide Dismutase Mimetic Surfaces to Reduce Accumulation of Reactive Oxygen Species for Neural Interfacing Applications. *J. Mater. Chem. B 2*, 2248−2258.
(123) Kolarcik, C. L., Bourbeau, D., Azemi, E., Rost, E., Zhang, L., Lagenaur, C. F., Weber, D. J., and Cui, X. T. (2012) In vivo effects of L1 coating on inflammation and neuronal health at the electrode−tissue interface in rat spinal cord and dorsal root ganglion. *Acta Biomater. 8*, 3561−3575.
(124) Azemi, E., Lagenaur, C. F., and Cui, X. T. (2011) The surface immobilization of the neural adhesion molecule L1 on neural probes

DOI: 10.1021/cn5002864
ACS Chem. Neurosci. 2015, 6, 68−83

and its effect on neuronal density and gliosis at the probe/tissue interface. *Biomaterials 32*, 681−692.
(125) Azemi, E., Stauffer, W. R., Gostock, M. S., Lagenaur, C. F., and Cui, X. T. (2008) Surface immobilization of neural adhesion molecule L1 for improving the biocompatibility of chronic neural probes: In vitro characterization. *Acta Biomater. 4*, 1208−1217.
(126) Zhong, Y., and Bellamkonda, R. V. (2008) Biomaterials for the central nervous system. *J. R. Soc., Interface 5*, 957−975.
(127) Bossi, S., Kammer, S., Dorge, T., Menciassi, A., Hoffmann, K. P., and Micera, S. (2009) An Implantable Microactuated Intrafascicular Electrode for Peripheral Nerves. *IEEE Trans. Biomed. Eng. 56*, 2701−2706.
(128) Smith, S. L., Judy, J. W., and Otis, T. S. (2004) An ultra small array of electrodes for stimulating multiple inputs into a single neuron. *J. Neurosci. Methods 133*, 109−114.
(129) Dymond, A. M., Kaechele, L. E., Jurist, J. M., and Crandall, P. H. (1970) Brain tissue reaction to some chronically implanted metals. *J. Neurosurg. 33*, 574−580.
(130) Eick, S., Wallys, J., Hofmann, B., van Ooyen, A., Schnakenberg, U., Ingebrandt, S., and Offenhausser, A. (2009) Iridium oxide microelectrode arrays for in vitro stimulation of individual rat neurons from dissociated cultures. *Front. Neuroeng. 2*, 16.
(131) Wei, X. F., and Grill, W. M. (2009) Analysis of high-perimeter planar electrodes for efficient neural stimulation. *Front. Neuroeng. 2*, 15.
(132) Frewin, C. L., Jaroszeski, M., Weeber, E., Muffly, K. E., Kumar, A., Peters, M., Oliveros, A., and Saddow, S. E. (2009) Atomic force microscopy analysis of central nervous system cell morphology on silicon carbide and diamond substrates. *J. Mol. Recognit 22*, 380−388.
(133) Jan, E., Hendricks, J. L., Husaini, V., Richardson-Burns, S. M., Sereno, A., Martin, D. C., and Kotov, N. A. (2009) Layered Carbon Nanotube-Polyelectrolyte Electrodes Outperform Traditional Neural Interface Materials. *Nano Lett. 9*, 4012−4018.
(134) Metz, K. M., Colavita, P. E., Tse, K.-Y., and Hamers, R. J. (2012) Nanotextured gold coatings on carbon nanofiber scaffolds as ultrahigh surface-area electrodes. *J. Power Sources 198*, 393−401.
(135) Wilks, S. J., Woolley, A. J., Liangqi, O., Martin, D. C., and Otto, K. J. (2011) In vivo polymerization of poly(3,4-ethylenedioxythiophene) (PEDOT) in rodent cerebral cortex. *EMBC, 2011 Annu. Int. Conf. IEEE*, 5412−5415.
(136) Abidian, M. R., Corey, J. M., Kipke, D. R., and Martin, D. C. (2010) Conducting-Polymer Nanotubes Improve Electrical Properties, Mechanical Adhesion, Neural Attachment, and Neurite Outgrowth of Neural Electrodes. *Small 6*, 421−429.
(137) Kuo, J. T., Kim, B. J., Hara, S. A., Lee, C. D., Gutierrez, C. A., Hoang, T. Q., and Meng, E. (2013) Novel flexible Parylene neural probe with 3D sheath structure for enhancing tissue integration. *Lab Chip 13*, 554−561.
(138) Kennedy, P. R., and Bakay, R. A. (1998) Restoration of neural output from a paralyzed patient by a direct brain connection. *NeuroReport 9*, 1707−1711.
(139) Kennedy, P. R., Mirra, S. S., and Bakay, R. A. (1992) The cone electrode: Ultrastructural studies following long-term recording in rat and monkey cortex. *Neurosci. Lett. 142*, 89−94.
(140) Kennedy, P. R. (1989) The cone electrode: A long-term electrode that records from neurites grown onto its recording surface. *J. Neurosci. Methods 29*, 181−193.
(141) Kennedy, P. R., Kirby, M. T., Moore, M. M., King, B., and Mallory, A. (2004) Computer control using human intracortical local field potentials. *IEEE Trans. Neural Syst. Rehabil. Eng. 12*, 339−344.
(142) Fan, W., Lee, T., Fujun, C., Kaplan, D., Berke, J., and Euisik, Y. (2013) A multi-shank silk-backed parylene neural probe for reliable chronic recording. *Transducers Eurosens. XXVII, Int. Conf. Solid-State Sens., Actuators Microsyst., 17th*, 888−891.
(143) Kozai, T. D. Y., Marzullo, T. C., Hooi, F., Langhals, N. B., Majewska, A. K., Brown, E. B., and Kipke, D. R. (2010) Reduction of neurovascular damage resulting from microelectrode insertion into cerebral cortex using in vivo two-photon mapping. *J. Neural Eng. 7*, 046011−046011.
(144) Zhang, H., Patel, P. R., Xie, Z., Swanson, S. D., Wang, X., and Kotov, N. A. (2013) Tissue-Compliant Neural Implants from Microfabricated Carbon Nanotube Multilayer Composite. *ACS Nano 7*, 7619−7629.
(145) Edell, D. J., Toi, V. V., McNeil, V. M., and Clark, L. D. (1992) Factors influencing the biocompatibility of insertable silicon microshafts in cerebral cortex. *IEEE Trans. Biomed. Eng. 39*, 635−643.
(146) Campbell, P. K., Jones, K. E., Huber, R. J., Horch, K. W., and Normann, R. A. (1991) A silicon-based, three-dimensional neural interface: manufacturing processes for an intracortical electrode array. *IEEE Trans. Biomed. Eng. 38*, 758−768.
(147) Bjornsson, C. S., Oh, S. J., Al-Kofahi, Y. A., Lim, Y. J., Smith, K. L., Turner, J. N., De, S., Roysam, B., Shain, W., and Kim, S. J. (2006) Effects of insertion conditions on tissue strain and vascular damage during neuroprosthetic device insertion. *J. Neural Eng. 3*, 196−207.
(148) He, W., and Bellamkonda, R. V. (2005) Nanoscale neuro-integrative coatings for neural implants. *Biomaterials 26*, 2983−2990.

DOI: 10.1021/cn5002864
ACS Chem. Neurosci. 2015, 6, 68−83